GUIDANCE DOCUMENTS ON MEASUREMENTS & MODELLING OF NOVEL AIR QUALITY POLLUTANTS:

OXIDATIVE POTENTIAL OF PARTICULATE MATTER

RI-URBANS

Research Infrastructures Services Reinforcing Air Quality Monitoring Capacities in European Urban & Industrial AreaS (GA n. 101036245)

By **with collaboration**

07/11/2024

RI-URBANS (http://www.RIURBANS.eu) is supported by the European Commission under the Horizon 2020 – Research and Innovation Framework Programme, H2020-GD-2020, Grant Agreement number: 101036245

Authors : Pamela Dominutti (CNRS), Jean-Luc Jaffrezo (CNRS), Roy Harrison (UoB), Xavier Querol (CSIC) & Gaëlle Uzu (CNRS)

Reviewers: Katriina Kyllönen (FMI), Elli Suhonen (FMI), Tuukka Petäjä (UHEL)

RI-URBANS (http://www.RIURBANS.eu) is supported by the European Commission under the Horizon 2020 – Research and Innovation Framework Programme, H2020-GD-2020, Grant Agreement number: 101036245

Table of Contents

ABBREVIATIONS

AA	Ascorbic acid
ACTRIS	Aerosols, Clouds and Trace gases Research InfraStructure
BB	Biomass burning
BBOA	Biomass burning organic aerosol
DCF	2,7-dichlorofluorescein
DCFH	Dichlorodihydrofluorescein
DTNB	Dinitrothiobenzoic acid
DTT	Dithiothreitol
EC	Elemental carbon
EEA	European Environment Agency
EPR	Electron Paramagnetic Resonance
ESR	Electron spin resonance
FOX	Ferric-xylenol orange
GSH	Glutathione
HPLC	High-performance liquid chromatography
HOA	Hydrocarbon-like organic aerosol
ILC	International interlaboratory comparison
LUR	Land Use Regression model
LV-OOA	Low volatile oxidized organic aerosol
MSA	Methanesulphonic acid
NAQD	New European Air Quality Directive (formally adopted 14th October 2024)
OC	Organic carbon
OP	Oxidative potential
OP^{AA}	Oxidative potential measured through the depletion of the ascorbic acid, a lung anti-oxidant
OP^{DTT}	Oxidative potential measured through the depletion of the dithiothreitol, a lung anti-oxidant's surrogate
OP^{GSH}	Oxidative potential measured through the depletion of the glutathione, a lung anti-oxidant
OP^{OH}	Oxidative potential measured through the formation of hydroxy radical
OP^{ESR}	Oxidative potential measured through the formation of particle-bound free radicals using electron paramagnetic resonance.
OPv	Extrinsic oxidative potential
PAH	Polyaromatic hydrocarbon
PCA	Principal component analysis
PM	Particulate Matter
PM1	Mass concentration of particles <1 µm
PM2.5	Mass concentration of particles <2.5 µm
PM10	Mass concentration of particles <10 µm
PMF	Positive Matrix Factorization, a receptor model for source apportionment
RI-URBANS	Research Infrastructures Services Reinforcing Air Quality Monitoring Capacities in European Urban & Industrial AreaS EU-project
ROS	Reactive oxygen species
SOP	Standard operation procedure
TNB	Trinitrobenzene
UA	Uric acid

CHEMICAL ELEMENTS & SPECIES

Cr	Chromium
Cu	Copper
Fe	Iron
H_2O_2	Hydrogen peroxide
K	Potassium
Mn	Manganese
Ni	Nickel
O_2^-	Superoxide radical
•OH	Hydroxyl radical
V	Vanadium
Zn	Zinc

1. ABOUT THIS DOCUMENT

This document was prepared as part of the "Research Infrastructures Services Reinforcing Air Quality Monitoring Capacities in European Urban & Industrial AreaS" (RI-URBANS) EU-project that connects the atmospheric observation expertise from Aerosols, Clouds and Trace gases Research InfraStructure (ACTRIS) with the urban air quality observation capacities of the regulatory air quality monitoring networks. It is specifically connected to the new European Air Quality Directive (NAQD) adopted on 14th October 2024.

The NAQD underlines the importance of emerging pollutants for AQ and the well-being of the citizens. Particularly, novel pollutants such as ultrafine particles (UFP), UFP-number size distribution (PNSD), black carbon (BC) and elemental carbon (EC), as well as ammonia (NH_3) and numerous volatile organic compounds (VOCs), and measurements of tracers of potential toxicity of PM (oxidative potential (OP) of particulate matter PM), are required or recommended to be monitored at both rural and urban supersites in order to support scientific understanding of their effects on health and the environment.

This **Service Tool (ST)** describes the steps needed to conduct measurements of **oxidative potential (OP) of atmospheric particulate matter (PM)**, and it provides an update on the state of the art on this harmonisation. This guidance document describes the different OP assays. It also provides information of the last studies comparing data and elucidates its connection with emission sources, chemical composition and size of PM. Furthermore, it gives recommendations to follow in the implementation of OP PM measurements according to the conclusions obtained in the first international interlaboratory comparison exercise developed in the framework of the RI-URBANS project. Finally, it shares a simplified measurement protocol developed for the most widely used **OP-dithiothreitol (DTT)** assay where the most critical steps have been optimised and harmonised in the framework of a dedicated task of RI-URBANS by a set of expert laboratories.

This is a RI-URBANS/ACTRIS guidance for this specific service tool that is part of the RI-URBANS deliverable D46 (D6.1, containing guidance for all service tools provided in the project) with the support for publication from AXA Research Fund to build up the final dissemination D55 (D7.6). Any dissemination of results must indicate that it reflects only the author's view and that the European Commission is not responsible for any use that may be made of the information it contains.

2. DEFINITION OF OXIDATIVE POTENTIAL OF PM

Health effects attributable to PM are complex and diverse, and overall, $PM_{2.5}$ is now considered to be the largest environmental contributor to adverse health effects globally (WHO, 2017). PM may act through different mechanisms such as oxidative stress and inflammation, genomic alterations, impaired nervous system function, epigenetic alterations, among others. Thus, it is not possible to cover all these effects by monitoring a single air quality parameter.

Oxidative potential of particulate matter (OP of PM) represents the capacity of PM to invoke oxidative reactions or to generate reactive oxygen species (ROS) in a biological media (Bates et al., 2015; Cho et al., 2005; Sauvain et al., 2008; Uzu et al., 2011). The ROS can be carried on by the PM or be induced/produced from their interactions with the biological system (e.g., fluids, cells, and tissues) and be quantified by different methodologies (Goldsmith et al., 1997; Landreman et al., 2008; Sarnat et al., 2016). Oxidative potential can be calculated for different target molecules, such as 1,4-dithiothreitol (OP^{DTT}), ascorbic acid (OP^{AA}), glutathione (OP^{GSH}), uric acid (OP^{UA}), and 2,7-

dichlorodihydrofluorescein (OP^{DCFH}), among the most used. These are known as depletion OP assays (Janssen et al., 2014; Shen et al., 2022). Furthermore, the (OP^{ESR}) assay measures OP based on the ability of PM to generate hydroxyl radicals (●OH) in the presence of hydrogen peroxide (H_2O_2), and the spin trap 5,5-dimethyl-1-pyrroline-N-oxide (DMPO) (Janssen et al., 2014), the OP^{OH} assay measures the formation of the radical hydroxyl (●OH) in surrogate lung fluid containing the major lung antioxidants, while the Electron Paramagnetic Resonance (EPR) assay measures particle-bound free radicals (Shen et al., 2022).

OP is usually a kinetic measurement based on the depletion rate of anti-oxidants or surrogates when in contact with PM. OP can be mass-normalised (OPm expressed in nmolAnti-Ox.min^{-1}.μg^{-1})) representing the inherent capacity of one µg of PM to oxidise the lung and is related the "harmfulness" of such PM. Or OP can be volume-normalised (OPv expressed in nmolAnti-Ox.min^{-1}.m^{-3})) related to the exposure of populations to atmospheric oxidant compounds. Note that OPv of PM is often abbreviated in OP of PM and OPm also called "intrinsic OP" in scientific literature.

2.1. Spatial and time variability of oxidative potential of PM

Oxidative potential activity from PM can vary based on the existence of emission sources, the chemical attributes of PM (e.g., speciation and solubility), as well as the size and surface area of the particle. It can be viewed as a comprehensive metric associated with particle toxicity through oxidative stress, as suggested by Calas et al. (2018). By relying on the concept that exposure to PM can trigger oxidative stress, OP of PM may contribute to identifying the particle characteristics accountable for certain observed health effects.

Oxidative potential activities can be measured by different acellular tests involving different anti-oxidants/surrogates (see further sections) that can give information about the intrinsic OP (mass normalised OP in nmol min^{-1} μg^{-1}) and the OP exposure (volume normalised OP in nmol min^{-1} m^{-3}).

The levels of OP of PM can vary from different places as they are affected by the chemical composition, the emission sources impacting PM, and the size and load of PM in each specific place. Over the last 10 years, very large improvements in source apportionment methods were developed to determine and quantify the main sources and processes influencing the PM measured at a given location. In addition, some other studies have focused on linking OP of PM to specific emission sources (Bates et al., 2019, and references therein) or establishing predictive regression models based on the concentrations of PM constituents (Weber et al., 2018; Weichenthal et al., 2016). Many studies have recently developed source apportionment techniques, such as principal component analysis (PCA), positive matrix factorization (PMF), random forest analysis and multilayer perceptron neural models (Borlaza et al., 2021; Daellenbach et al., 2020; Grange et al., 2022; in 't Veld et al., 2023; Shen et al., 2022; Srivastava et al., 2018; Weber et al., 2021, 2019).

Due to the seasonality of emissions sources (e.g. biomass burning in winter), some studies report strong differences between seasons related to the main emission sources driven OP, whereas others do not (Borlaza et al., 2021; Calas et al., 2019; Cesari et al., 2019; Dominutti et al., 2023; Paraskevopoulou et al., 2019; Perrone et al., 2016; Pietrogrande et al., 2018; Zhou et al., 2019). In general, those studies performed in regions with strong seasonal changes (i.e., mountainous areas) presented higher dissimilar source contributions than those located in temperate areas (i.e., coastal areas). Additionally, several studies have already shown that different sources of PM have different sensitivities to OP tests (Bates et al., 2015; Cesari et al., 2019; Daellenbach et al., 2020; Dominutti et al., 2023; Fang et al., 2016; Paraskevopoulou et al., 2019; Verma et al., 2014; Weber et al., 2018; Zhou et al., 2019). In particular, sources with high concentrations of transition metals, such as road traffic, road dust and industrial sources, seem to have a higher intrinsic potential than other PM sources for a given OP. Nevertheless, there is still a limited number of studies integrating long-term PM monitoring and they only sometimes consider seasonal variability. Consequently, they may not encompass a comprehensive variability of emission sources for a given site, omitting some important features on the source-related OP of PM. This limitation is even higher in terms of spatial

distribution. Most of the studies were developed in high-income regions, where the discrepancies related to emission sources are less significant.

Finally, attaining a general model linking OP of PM with site-specific PM constituents or emission sources is challenging because OP depends not only on the concentrations of redox-active species but also on factors that influence the diversity of redox reactions and the formation of ROS in the human body (Shahpoury et al., 2022). Thus, the selection of the OP assays to obtain a wide range of OP determinants will depend on previous knowledge about the PM characteristics for a given location. Combining two or three OP assays with complementary sensitivities will provide more exhaustive information about the PM characteristics underlying the OP effects on human health.

2.2. Links of oxidative potential of PM and health outcomes

Research on OP of PM started in 2005, and considerable efforts have been put into developing measurement protocols and linking this new parameter to PM compounds, their emission sources and adverse health effects. Improvements in recent years in high-throughput offline techniques and online OP of PM devices, as well as in the apportionment of OP of PM among PM sources, will have a significant impact on targeting emission sources that are the key to creating lung oxidative damage and reducing the health effects of air pollution. The added value of OP of PM appears to be an essential property of particles which constitutes a unifying factor between the PM sources and their effects on health.

Recently, OP of PM and its related sources have been linked to certain health outcomes. Nevertheless, clear evidence of OP of PM as a satisfactory proxy of specific health outcomes is still needed, and there is so far no consensus toward a standardised method to measure the OP of PM. In the last years, increased evidence has associated OP^{DTT} and OP^{AA} assays with health endpoints (Bates et al., 2015; Borlaza et al., 2022; Canova et al., 2014; Fang et al., 2017b; Janssen et al., 2015; Marsal et al., 2023; Strak et al., 2017; Weichenthal et al., 2016; Yang et al., 2016). Some studies have evaluated the associations between OP assays and health endpoints, using OP of PM observations and modelling approaches, such as land-use regression models (LUR), to evaluate the OP of PM spatial variability when measurements were unavailable (Bates et al., 2015; Gulliver et al., 2018; Strak et al., 2017).

Numerous studies using the OP^{AA} assay exhibited no correlation with adverse health endpoints, encompassing early-life outcomes, respiratory and cardiovascular mortality, cardiorespiratory emergencies, and lung cancer mortality (Borlaza et al., 2022; Fang et al., 2017a; Maikawa et al., 2016; Marsal et al., 2023; Weichenthal et al., 2016). Nevertheless, certain positive associations were identified between OP^{AA} and systemic inflammatory biomarkers, as well as for OP^{ESR}, in studies focused on short-term exposure (Janssen et al., 2015; Liu et al., 2018; Marsal et al., 2024). These findings suggest that OP^{AA} provides limited insights into the connection between OP PM and adverse health effects. However, the existing body of studies is insufficient to rule out its predictive capacity for health outcomes. Studies by Korsiak et al. (2022) and Toyib et al. (2022) established strong associations between outdoor fine particles, oxidising gases, respiratory hospitalisations of children and mortality when levels of metals, sulphur and OP PM (especially for OP^{GSH} and, in specific cases, OP^{AA}) were elevated.

On the other hand, two thiol-base probes have shown more positive associations with health. OP^{DTT} has been linked with various acute cardiac (e.g., myocardial infarction) and respiratory endpoints in several studies (Abrams et al., 2017; Bates et al., 2015; Delfino et al., 2005; Fang et al., 2017b, 2016; He et al., 2021; Janssen et al., 2015; Weichenthal et al., 2016; Yang et al., 2016). A Canadian cohort (193,000 participants) showed some significant association between OP^{GSH} and cause-specific mortality as well as lung cancer (Weichenthal et al., 2016). Recently, as a result of a long-term cohort study, Marsal and co-workers have shown a consistent association between personal prenatal OP^{DTT} and several early-life lung function parameters related to lung growth restriction (Marsal et al., 2023). Such findings are aligned with pioneering studies using the PIAMA (Prevention and Incidence of Asthma and Mite Allergy) birth cohort to show that respiratory health was more strongly associated with OP^{DTT} than with $PM_{2.5}$ mass (Yang et al., 2016). Similarly, two cohort studies found some positive associations between personal

OP of $PM_{2.5}$ and foetal growth restrictions, specifically decreased weight and height at birth were correlated with OP^{DTT} and OP^{GSH} (Borlaza et al., 2022; Lavigne et al., 2018). Overall, a key point of most of the previously reported studies is that OP of PM was more predictive for health outcomes than other components, including PM mass.

Finally, one study with the emerging OP assay assessing a direct radical •OH measurement in the lining fluid found some positive associations for OP^{OH} and asthma, cardiovascular disease and low birth weight (also seen for OP^{DTT}) in Los Angeles (Shen et al., 2022). As for OP^{ESR}, further studies involving OP^{OH} are needed to assess some statistics on such methodologies that are promising.

These studies increase evidence about the relevance of OP of PM as a useful health-based exposure metric. They also promote the use of OP assays relying on antioxidant thiol-based probes with a wide and balanced sensitivity to PM compounds: OP^{DTT} and OP^{GSH} are to date the most promising OP assays (with probably still a small advantage for OP^{DTT} due to its wider application in more epidemiological studies for being the oldest assay) but other assays cannot be ruled out. Overall, epidemiological evidence remains limited because this field of research is relatively recent. The application of OP of PM in health studies has been enabled very recently (less than 10 years), with the emergence of less time-consuming OP methodologies. Nevertheless, these studies have to be done with standardised OP of PM protocols to inform about the capacity of OP of PM to be an additional health predictor with PM mass and how the PM characteristics and the different OP assays can link the acute and chronic health effects associated with air pollution.

3. MEASUREMENT METHODS OF OXIDATIVE POTENTIAL OF PM AND QUALITY CONTROL

3.1. Harmonisation of measurement methods

There has not been a harmonised OP of PM measurement protocol developed so far. All the groups are using their own protocol based on different probes or different step regarding the extraction, or the measurement itself, making the measurements not comparable worldwide.

Even if several OP acellular assays have been developed and there has been many improvements in the state of knowledge of OP assays in recent years, further developments are still needed to achieve standardisation of the different OP tests. This is compulsory to reach a scientific consensus for comparison purposes and to allow wide and accurate use of this measure. For this purpose, a group of EU researchers within EU RI-Urbans project set up a simplified and harmonised protocol for one OP assay, the OPDTT protocol (named OPDTT RI-URBANS' SOP) to launch the first international interlaboratory comparison exercise. The following sections develop the current recommendations for OP assays, the associated OPDTT RI-URBANS' SOP and the results of the intercomparison.

3.2. Description of the available methods and protocols

As an indicator of PM oxidative properties, OP of PM has been measured to reflect the capability of PM to generate ROS either through the consumption of antioxidants or the production of oxidants during the process of PM interactions with the biological system (Goldsmith et al., 1997; Landreman et al., 2008). OP of PM can be assessed offline on atmospheric samples or online (to date only research prototypes are available). This service tool focuses on offline measurements from filter samples that are extracted into liquid suspension (several procedures co-exist) before being submitted to the following different assays.

Two types of methods have been used to measure OP of PM, including cellular assays and acellular assays. Commonly used acellular assays include the use of lung anti-oxidants or surrogates such as DTT, AA, GSH, UA, and DCFH and are consequently called $OP^{Anti\text{-}Ox}$. Specifically, OP^{DTT}, OP^{AA}, OP^{GSH} assay involved the incubation of the antioxidants (DTT, AA, GSH) in PM aqueous extracts in water, methanol, or simulated lung fluid (Calas et al., 2017) and the loss (depletion) rate of the antioxidants provided an estimation of OP PM (Massimi et al., 2020). In contrast,

the DCFH method was based on the reaction of the ROS in PM with DCFH, a non-fluorescent reagent, with the presence of horseradish peroxidase. This reaction produced a fluorescent compound, 2,7-dichlorofluorescein (DCF). Because not all oxidants can react with DCFH, the intensity of the fluorescence generated from the reaction did not necessarily capture the total oxidative capacity and provided a proxy of OP of PM (Massimi et al., 2020; Perrone et al., 2016). Similar to the OP^{DCFH} assay, two other methods were developed to measure the continuous generation of ROS over time, using high-performance liquid chromatography (HPLC) with fluorescent probes and electron spin resonance (ESR) (Bates et al., 2019). In particular, ESR measures PM-induced hydroxyl radical (•OH) formation by detecting the electron paramagnetic resonance (EPR) signals (Hellack et al., 2014; Shi, 2003). HPLC methods measure a series of substances that are generated by the reaction of ROS with specifically selected chemicals for the assay (Shen et al., 2011). It has been reported that different acellular assays focused on different redox reactions. For example, the ESR and HPLC methods were more sensitive to specific ROS, including H_2O_2 and OH, while the OP^{DTT} assay was more sensitive to hydrogen peroxide (H_2O_2) and superoxide radical (O_2^-) (Bates et al., 2019; Xiong et al., 2017). On the other hand, the AA and GSH assays were not specifically responsive to a particular ROS (Bates et al., 2019). Similarly, DCFH reacts with multiple ROS, including •OH and H_2O_2 (Bates et al., 2019). The focus on different redox reactions could be a major reason leading to differences in method performance. For example, the OP examined by the OP^{AA} assay and the OP^{GSH} assay on the same PM samples only had a moderate Pearson correlation (r^2 =0.43–0.45) (Maikawa et al., 2016).

3.3. Recommendations for measurements of oxidative potential of PM.

The recommendations summarised here are obtained from the studies done in the framework of RI-URBANS and published by Dominutti et al. (2024).

3.3.1 Sampling, preservation and treatments prior to the analysis

OP measurements of PM are currently mostly made offline with filter samplers collected and accumulating sample for a given period of time. Sampling of filters can be done with Teflon filters or quartz filters using low-volume/high volume impactors or according EN 12341 ensuring a minimal load of PM enabling to get a 25µg.ml^{-1} extraction concentration. The OP analysis also requires some field blank to remove some potential contamination and matrix effect.

Nevertheless, OP of PM can be also assessed online but to date only research prototypes are available. This Service Tool focuses on offline measurements from filter samples that are extracted into liquid suspension (several procedures co-exist) before being submitted to the following different assays.

It goes without saying that not only the preparation, but also the conservation, of the samples before incubation affect the OP results. Accordingly, PM filter samples **have to be preserved frozen (or kept at ≤4°C cold if the analysis is fast after collection) from the sampling to the analysis to prevent losing reactive species**. In addition of the preservation before analysis, the protocol for extracting PM fractions from the filters is also a key parameter to harmonise. PM can be extracted using water, methanol or lining fluid; with diverse time, ultrasounds, vortex or gentle agitation. This step needs further standardisation, but to date, we can recommend an extraction to be the closest to lung physiological conditions i.e. water-based (ultrapure water or water-based buffer or water-based simulated lining-fluid) at pH7.4, and 37.4°C with a vortex-extraction during 75 min to extract all PM compounds. Sonication is less recommended than vortex extraction because it is known to create some extra-ROS in the media. Then, assays involve obtaining filtered PM extract (water-soluble OP) or unfiltered PM suspensions (total OP including water-soluble and insoluble fractions) to subsequently incubate these with chemical reagents that influence the response. Because, PM comes in contact with the lungs with soluble and insoluble compounds, we recommend to assess OP with unfiltered PM suspension to take both soluble and insoluble fraction into account. When using different protocols and conditions, discrepancies in OP measurements might be obtained and this crucial step need further standardisation (Calas et al., 2018; Yang et al., 2014).

3.3.2 The type of recommended assays

As shown in prior sections there are different OP assays. The selection of these will influence the PM source contributions that will govern OP of PM values with the selected assay. Thus, OP^{AA} probably will be more affected by specific metals and few specific organics, while OP^{DTT} is influenced by a wider range of contributions. Accordingly one has to bear in mind that the choice of the OP assay affects the ranking of the OP of the PM source exposure, which can complicate the message to deliver to local stakeholders for mitigation actions (Dominutti et al., 2023; Gao et al., 2020). **However, the future choice of the best OP assay (or combination) does not depend on the link done with PM compounds and sources but on health evidence**.

Currently five, but mainly three, OP assays have been evaluated in terms of health outcomes. Until now, little evidence was found between OP^{AA} and diseases observed in populations despite some associations with biomarkers of inflammation (Marsal et al., 2024). There is also a lack of studies to be conclusive for emerging direct OP assays (OP^{OH} and ^{OPESR}), even if they look promising (Yang et al., 2016). This is why, in the absence of other assays with a sufficient number of studies, thiol-based OP assays, namely OP^{DTT} and OP^{GSH}, emerge as the most promising OP assays regarding health evidence (Abrams et al., 2017; Borlaza-Lacoste et al., 2024; Fang et al., 2016; Janssen et al., 2015; Weichenthal et al., 2016; Yang et al., 2016). These evidences are sufficient to recommend additional routine monitoring on a larger temporal and spatial scale. Routine monitoring will greatly enhance the power of epidemiological studies, further investigating the link between OP of PM and health. To be more informative, it would be essential to simultaneously monitor more traditional air pollution metrics such as $PM_{2.5}$, PM_{10} and NO_2 to evaluate the additional value of OP of PM.

Here we recommend **at least two complementary and simultaneous assays, a thiol-based probe (OP^{DTT} or OP^{GSH}) and another one (among OP^{OH}, OP^{AA}, or else) to capture insight from a wide range of redox-active species**. Currently, we consider that this will assess the complete picture of the most oxidising PM compounds/sources, and will better allow evaluating their relation to health effects. Finally, the selection of the complementary OP tests to be applied in a given place needs to be wisely evaluated and will strongly depend on the previous knowledge about the geochemistry of sources, concentrations and chemical composition of PM evaluated. Such a strategy is also essential since this affects the message to be delivered about the targeted sources in future mitigation policies.

Regarding the use of a protocol, OP^{DTT} protocol was simplified and harmonised during RI-URBANS project, and the detailed protocol can be found below

*3.3.3 Harmonised and simplified OP^{DTT} protocol (**OP^{DTT} RI-URBANS' SOP**) «Evaluation of acellular reactivity of particles by dithiothreitol (DTT) assay»*

3.3.3.1 Method 1 – OP DTT assay using plate readers

Before the absorbance measurements of the samples, perform a calibration of your analytical device using a DTT calibration curve for a concentration range between 0 and 60 µM (titration with 1mM DTNB and reading of TNB formation at 412 nm) and report the results on the Excel file provided.

3.3.3.2 Reagents

3.3.3.2.1 Preparation of potassium phosphate (0.1 M) buffer solution at pH 7.4

Weight 13.41 g of dipotassium phosphate (K2HPO4, CAS [7758-11-4]) and 3.13 g of potassium dihydrogen phosphate (KH2PO4, CAS [7778-77-0]) and mix them in a volumetric flask of 1000 mL with ultra-pure MilliQ water. Check the pH using a pH meter; the reading should be equal to 7.4 ± 0.1.

3.3.3.2.2 Preparation of DTT mother solution (8.3 mM)

Weight 38.6 mg of 1,4-Dithiothreitol (DTT, CAS [3483-12-3]) and add 30 ml of potassium phosphate buffer solution (A2.1). Keep the solution under an ice bath or in the fridge until use.

3.3.3.2.3 Preparation of DTT daughter solution (0.25 mM)

This solution is obtained from 1.20 mL of the 8.3 mM DTT solution (A2.2) and completed to a final volume of 40 ml with potassium phosphate buffer solution (A2.1). Keep the solution under an ice bath or in the fridge until use.

3.3.3.2.4 Preparation of Dinitrothiobenzoic acid (DTNB) mother solution (10 mM)

Weight 118.8 mg of 5,5'-Dithiobis (2-nitrobenzoic acid) (DTNB, CAS [69-78-3]) and add 30 ml of the potassium phosphate buffer solution (A2.1). Keep the solution under an ice bath or in the fridge until use.

3.3.3.2.5 Preparation of DTNB daughter solution (1 mM)

This solution is obtained by diluting 4mL of the 10mM DTNB solution (A2.4), completing a total volume of 40 mL with the potassium phosphate buffer solution (A2.1). Keep the solution under an ice bath or in the fridge until use.

3.3.3.3 Particulate Matter suspension solutions to be tested - samples

Example given below for the analysis of 4 PM samples extracted at 25 µg.mL in physiologically conditions (pH7.4, 37,5°C) and unfiltered.

3.3.3.4 Material

One transparent 96-wells plate is sufficient to process all the samples in triplicate. You can use a separate 96-wells for the calibration curve of DTT.

The samples need to be under agitation during the experiment time at 37.4°C.

An ice bath is required to keep the DTT and DTNB cold (at least keep the reagent solution fresh in the freezer until use).

3.3.3.5 Procedure for plate readers automatically injected

DTT Exposure and DTNB analysis

Set up the temperature of the plate reader at 37.4°C for the duration of the assay.

1. Draw up a grid for 96-wells plate and locate the samples SP1 to SP4 as in the table below, leaving the first 3x4 wells for the controlox (inherent DTT background oxidation).

	1	2	3	4	5	6	7	8	9	10	11	12	
A	Controlox	Controlox	Controlox	SP1	SP1	SP1	SP2	SP2	SP2	SP3	SP3	SP3	**T=0**
B	Controlox	Controlox	Controlox	SP1	SP1	SP1	SP2	SP2	SP2	SP3	SP3	SP3	**T=10**
C	Controlox	Controlox	Controlox	SP1	SP1	SP1	SP2	SP2	SP2	SP3	SP3	SP3	**T=20**
D	Controlox	Controlox	Controlox	SP1	SP1	SP1	SP2	SP2	SP2	SP3	SP3	SP3	**T=30**
E	SP4	SP4	SP4										**T=0**
F	SP4	SP4	SP4										**T=10**
G	SP4	SP4	SP4										**T=20**
H	SP4	SP4	SP4										**T=30**

2. Place 20 µL of samples SP1 to SP4 into each well and 20 µl of ultrapure water in Controlox wells.
3. Add 220 µL of the potassium phosphate buffer solution (A2.1) in the sample wells SP1 to SP4 and in the control wells.
4. Set up the plate reader at 37.4oC.
5. Place the plate into the reader and incubate for 10 minutes.

6. Shake the plate by the instrument for one minute.
7. Read the intrinsic absorbance of the samples/control at 412 nm.
8. At T= 0 min, program the injector A to dispense 50µL of 0.25 mM DTT (A2.2) in ALL wells. Keep the solution under an ice bath or in the fridge until use.
9. At T=0 min, program injector B to dispense 50µL of 1 mM DTNB (A2.5) into the T=0 wells (lines A and E). Keep the solution under an ice bath or in the fridge until use.
10. Shake the plate by the reader for 30 seconds every minute for 10 minutes.

At T=10 minutes, dispense 50 µL of 1 mM DTNB (A2.5) into the T=10 wells (lines B and F) to stop the DTT consumption reaction by the samples.

11. Shake the plate by the device for 30 seconds every minute for 10 minutes.

At T=20 minutes, dispense 50 µL of 1 mM DTNB (A2.5) into the T=20 wells (lines C and G).

12. Shake the plate by the device for 30 seconds every minute for 10 minutes.

At T=30 minutes, dispense 50 µL of 1 mM DTNB (A2.5) into the T=30 wells (lines D and H).

13. Shake the plate for 60 seconds, wait 10 seconds and read the final absorbance at 412 nm. The yellow compound (TNB) formed is stable for two hours; only one final absorbance measurement is necessary.
14. Calculate the kinetics of the DTT oxidation as:
    - nmol DTT/min is obtained by subtracting both the intrinsic absorption of each sample (to remove a potential matrix effect between samples, the value obtained in step 7) and the inherent DTT auto-oxidation rate (slope of Controlox sample) from the DTT consumption rate in the presence of particles (SP1-4).
    - nmol DTT/min/µg is obtained by subtracting both the intrinsic absorption of each sample and inherent DTT auto-oxidation rate from the DTT consumption rate in the presence of particles and dividing it by the mass of particulate matter in the reaction.
    - % DTT consumed/ug/min is obtained by the % of DTT lost over the reaction with samples relative to the inherent DTT auto-oxidation and normalised by the reaction time and per µg of PM.
    - All these formulas are pre-included in the Excel spreadsheet provided.
    - Use it to add the results using your lab reference number, the analytical protocol and instrument used and the reference number for each sample.

3.3.3.6 Procedure for plate readers without injectors

DTT Exposure and DTNB analysis:

Set up the temperature of the plate reader at 37.4°C for the duration of the assay.

1. Draw up a grid for 96-wells plate, and locate the samples SP1 to SP4 as in the table above, leaving the first 3x4 wells for the control sample (inherent DTT background oxidation).
2. Place 20 µL of samples SP1 to SP4 into each well and 20 µl of ultrapure water in Controlox wells.
3. Add 220 µL of the potassium phosphate buffer solution (A2.1)) in the sample wells SP1 to SP5 and in the control sample wells.
4. Introduce the plate into the reader and read the intrinsic absorbance of the solutions at 412 nm.
5. Inject 50 µL of 1mM DTNB (A2.5) into the T=0 min wells (lines A and E) (this is done to avoid depletion of DTT with samples at t=0 with manual injection, which is slower than injectors). Keep the DTNB solution under an ice bath or in the fridge until use.
6. Dispense 50 µL of 0.25 mM DTT (A2.2) in ALL wells. Keep the DTT solution under an ice bath or in the fridge until use.
7. Set up the plate reader at 37.4 oC.
8. Introduce the plate into the plate reader and incubate for 10 mins.
9. Shake the plate by the device for 30 seconds every minute for 10 minutes.

At T=10 minutes, remove the plate from the instrument and inject 50 µL of 1mM DTNB (A2.5) into the T=10 wells (lines B and F) to stop the DTT consumption reaction by the samples.

10. Place the plate back on the reader and stir it for 30 seconds every minute for 10 minutes.At T=20 minutes, remove the plate from the reader and inject 50 µL of 1mM DTNB (A2.5) into the T=20 wells (lines C and G).
11. Place the plate back on the reader and shake it for 30 seconds every minute for 10 minutes.

At T=30 minutes, remove the plate from the reader and dispense 50 µL of 1mM DTNB (A2.5) into the T=30 wells (lines D and H).

12. Place the plate back into the reader and shake it for 60 seconds, wait 10 seconds and read the final absorbance at 412 nm. The yellow compound (TNB) formed is stable for two hours; only one final absorbance measurement is necessary.
13. Calculate the kinetics of the DTT oxidation as:
    - nmol DTT/min is obtained by subtracting both the intrinsic absorption of each sample (to remove a potential matrix effect, value obtained in step 4) and the inherent DTT auto-oxidation rate of the blank (slope of Controlox sample) from the DTT consumption rate in the presence of particles (SP1-4).
    - nmol DTT/min/µg is obtained by subtracting both the intrinsic absorption of each sample and inherent DTT auto-oxidation rate from the DTT consumption rate in the presence of particles and dividing it by the mass of particulate matter in the reaction.
    - % DTT consumed/ug/min is obtained by the % of DTT lost over the reaction with samples relative to the inherent DTT auto-oxidation and normalised by the reaction time and per µg of PM.
    - All these formulas are pre-included in the Excel spreadsheet provided.
    - Use it to add the results using your lab reference number, the analytical protocol and instrument used and the reference number for each sample.

3.4. Results from the first oxidative potential inter-laboratory comparison

The RI-URBANS ILC was proposed to evaluate the discrepancies and commonalities of OP measurements obtained by the different participating laboratories. It was decided to prioritise the OP^{DTT} assay for such first attempt of an international intercomparison due to its widespread adoption and longevity in the research community. This choice aims to facilitate broad participation from laboratories in the research field. The ILC exercise was performed using three samples (samples 1, 2 and 3), including different concentrations of ambient PM and commercial positive control (Naphthoquinone), all extracted in ultra-pure water prepared by the reference laboratory.

A total of 20 research groups participated in the exercise: 14 of them from Europe, including the United Kingdom, Italy, France, Switzerland, Greece, Germany, Serbia, Czech Republic, Netherlands and Sweden, 3 groups from the United States, 2 groups from Canada and 1 from Australia. The participants were invited for their contribution to the RI-URBANS project through a public call launched at the IAC conference in Athens (in September 2022) due to their active role in the OP scientific community or because they contacted the reference laboratory directly. The exercise asked for anonymous participation; thus, the number randomly assigned to each laboratory/group will be used to present the results.

Participants were asked to report OP^{DTT} results according to the RI-URBANS' SOP for each of the samples in three replicates in specified units (nmol DTT min-1 µg-1) with three decimal digits. In addition, participants were invited to report, under the same format, the values for other OP tests, such as OP^{DTT}, OP^{AA}, OP^{DCFH}, OP^{OH}, OP^{ESR}, OP^{GSH} (routinely applied by each group) on the same samples.

Each participant (total 21 laboratories) reported the results using the RI-URBANS' OP^{DTT} SOP for the three different samples (samples 1 to 3) in triplicates. Assigned values for each sample were obtained from the average results obtained from a particular number of participants, selected (without knowing their results) due to their previous pioneering experience in developing OP protocols and measurements, taken as a strong expertise in the domain (>10 publications in the field).

The assessment of laboratory performances integrated the bias in results across participant groups compared to the assigned values and their associated standard deviation for each sample. Sample 1 exhibited the highest

variances, ranging from 130% to -35%, with only 5 groups displaying differences within ±10%. For Sample 2, differences were within a narrower range from 43% to -7%, primarily favouring overestimations. For this sample, 12 participants returned results that were within ±10% of the assigned value. Finally, the results for Sample 3 demonstrated the least variation among participants, with differences ranging from 30% to -6%, and 16 participants within ±10% of the assigned value, again favouring overestimation compared to the assigned value. It is interesting to note that there is apparently no systematic pattern where a given participant would obtain out-of-range results for all samples. The results are really contrasted, and most participants could obtain "good" results for one or two samples associated with one "outlier". This underscores the need for further investigations on the causes of the variations observed, possibly in the next ILC.

The ILC results were statistically analysed by the European Joint Research Centre, which provides independent, evidence-based science and knowledge to support EU policies and conducting ILC in general.

The individual performance of each group was further evaluated using z-scores, a metric indicating the deviation of each data point from the assigned value. For each laboratory and test sample, the z-score is computed using the formula: $z = (x_i - X)/\sigma^*$, where x_i is the result from participant i, X is the sample assigned value, and σ^* is the standard deviation of the assigned value. An "action signal" is triggered if a participant's entry produced a bias exceeding z=+3 or falling below z=-3, indicating a deviation of more than 3 standard deviations from the assigned value. Similarly, a "warning signal" is raised for a laboratory bias above z=+2 or below z=-2, representing a deviation between 2 and 3 standard deviations. A laboratory bias between z=-2 and z=+2 signified satisfactory performance concerning the standard deviation for proficiency assessment.

The results are presented in Figure 1. Some of the same observations as above can be made. First, all the underestimations fell within the acceptable range. Second, it is noteworthy that no laboratory exhibited unsatisfactory performances across all three samples; for virtually all participants, while one sample could present poor results, it coexisted with two acceptable ones. Again, this calls for explanations that are not systematic biases in the analyses. While factors like sample inhomogeneity may be at play (particularly for Sample1), some other issues, including variability in the handling of the analysis, may have had an impact. Hence, participants exhibiting significant deviations (|z-scores| > 2) for some of their results should thoroughly examine their procedures and possibly implement appropriate corrective actions to avoid similar outcomes in future interlaboratory comparisons. **However, overall, half of the participants achieved results within the acceptable limits of this test. Despite disparities, these findings are really promising, especially considering that this is the first-ever exercise of its kind** (Dominutti et al., 2024). Such results are similar to those obtained for some of the first ILCs for PAHs (Grandesso et al., 2012; Verlhac et al., 2014), for example.

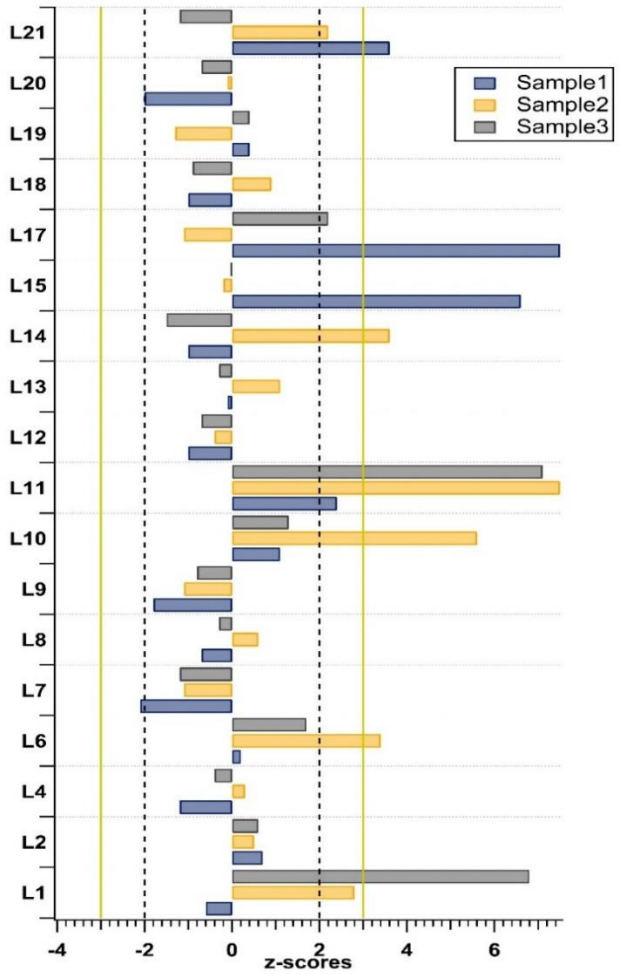

Figure 1. *Z-scores obtained to evaluate each participant's performance in the interlaboratory comparison for each sample tested following the RI-URBANS* OP^{DTT} *SOP (adopted from Dominutti et al., 2024).*

3.5. Data management

For now, this is non-applicable since the OP of PM monitoring data is still not produced at the European level. The data is collected by individual research groups and has been made available in several scientific publications. It is expected that reporting of OP of PM data will be made possible in the next years by, e.g., European Environment Agency (EEA).

4. PAN-EUROPEAN OVERVIEW OF OXIDATIVE POTENTIAL OF PM

4.1. Oxidative potential of PM in urban Europe

In recent years, there has been an increase in studies examining the OP of PM across Europe. Reactive oxygen species associated with PM are suspected of inducing oxidative stress in vivo, potentially leading to adverse health effects such as respiratory and cardiovascular diseases. Despite suggestions that oxidative potential plays a significant role in the acute health impacts of PM, the precise link remains unclear. Investigations into which components of PM exhibit oxidative activity have produced contrasting findings, leaving much yet to be understood about the sources of PM that may influence their relative OP. Consequently, there is growing interest in exploring

the health risks associated with PM exposure by examining OP of PM, particularly in the European context. In this discussion, we delve into the primary findings collected from studies conducted in the region.

A study in Spain (In 't Veld et al., 2023) included the evaluation of PM_{10}, $PM_{2.5}$, and PM_1 samples collected roughly every four days at an urban background site and a rural background site. This is one of the few studies in Europe evaluating the OP of PM at three different PM sizes over one year and also comparing two different site typologies. The assessment of the chemical composition of PM samples allows the application of source apportionment using PMF to identify the main PM sources. Regarding OP of PM, the parameters OP^{DTT} and OP^{AA} of PM were determined. Finally, to link the sources with the measured OP of PM, multiple linear regression models were applied to the datasets. The findings revealed that in Barcelona, OP of PM_{10} was notably higher compared to that of $PM_{2.5}$ and PM_1. Conversely, at the rural site, the results across all PM sizes were within a similar range but notably lower than those observed in the urban site. In the urban area, various anthropogenic sources emerged as the primary influencers of OP in PM_{10} (including combustion, road dust, heavy oil, and sources rich in organic carbon) and $PM_{2.5}$ (road dust and combustion). In contrast, the rural site showed no distinct factors influencing OP of PM evolution, which likely accounts for the absence of a notable difference in OP among PM_{10}, $PM_{2.5}$, and PM_1. This study underscored the importance of size fractions in determining OP depending on the environmental context. In urban settings, OP of PM is influenced by both PM_{10} and PM_1 size fractions, whereas in rural environments, only the PM_1 fraction is significant (in 't Veld et al., 2023).

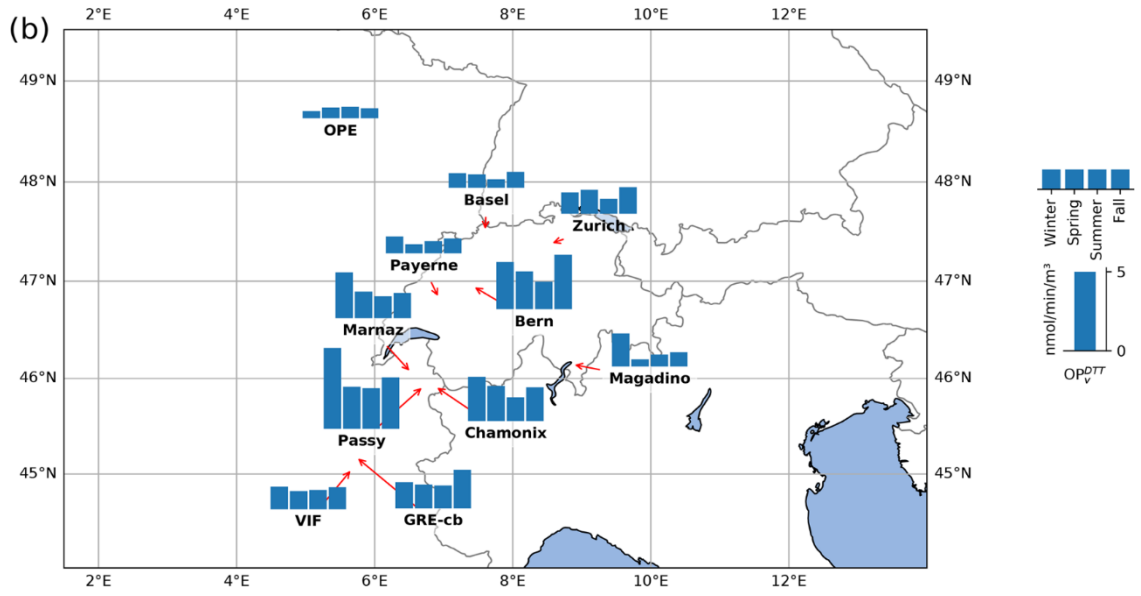

Figure 2. *Seasonal volumic OP^{DT}vmeans for the five Swiss sites included in this analysis and the closest six French sites surrounding Switzerland. Data from the French sampling sites are from Weber et al. (2021) and Grange et al. (2022).*

Similarly, an intensive PM and OP of PM sampling campaign conducted across Switzerland sites between 2018 and 2019 demonstrated that OPv was variable in time and space as illustrated in Figure 2 (Grange et al., 2022). OPv patterns reflected the typical distribution of atmospheric pollutants, with urban areas exhibiting higher pollution levels compared to rural regions, especially during wintertime. Despite notable differences in PM mass between rural and urban locations, OP metrics consistently displayed even greater variation, indicating a higher level of heterogeneity in OP of PM compared to PM mass across the sampling sites in Switzerland. The results exhibited more pronounced seasonal variations for OP^{AA} and OP^{DTT} assays compared to the third OP^{DCFH} assay, making the former approaches more useful for data analysis. PM_{10} and $PM_{2.5}$ sources identified by PMF models highlighted two major anthropogenic emission sources, namely road traffic and wood combustion as significant drivers of OP in the country. In contrast, secondary inorganic nitrate and sulphate sources generally displayed low levels of "intrinsic OP" (OP normalised per µg of particles, OPm) across Switzerland. This suggested a potential discrepancy between the total PM mass concentration and OPm, prompting a shift in management priorities towards addressing health

impacts rather than focusing solely on the total mass. While the causality of identified sources in driving OPv warrants further investigation into biological mechanisms, the results align with existing literature and provide clear guidance on where future research efforts should be directed. Additionally, the distinct characteristics of OPv in PM_{10} and $PM_{2.5}$ size fractions emphasised the importance of continued monitoring, particularly for coarse-mode particles (Grange et al., 2022).

In the last years, some advances in OP studies were related to the use of modelling tools to better understand the spatial variability of the OP of PM linked to the emission sources of PM (Figure 3). In the study of Daellenbach (2020), the authors used field observations and air-quality modelling to assess the primary and secondary origins of PM and OP PM across Europe. The main findings were in line with the results observed in Switzerland (Grange et al., 2022), which revealed that the mass concentration of PM is predominantly influenced by secondary inorganic components, crustal material, and secondary biogenic organic aerosols. In contrast, anthropogenic sources, notably fine-mode secondary organic aerosols from residential biomass burning and coarse-mode metals from vehicular non-exhaust emissions, were the primary contributors to OP activities.

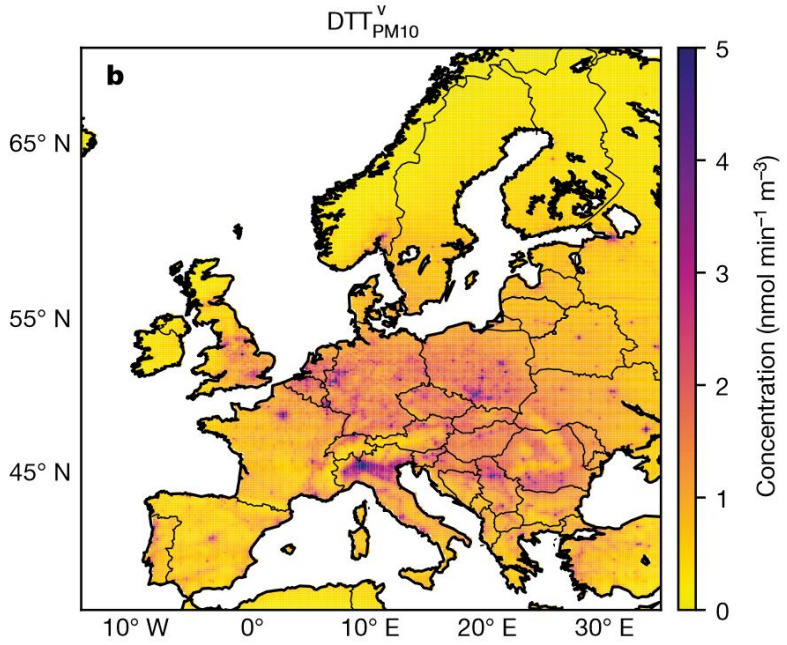

Figure 3. *Levels of OP^{DTT}v of PM10 in Europe. OPv in Europe for the year 2011 (adopted from Daellenbach et al., 2020).*

Similar results were also obtained from the OP PM measurements conducted using two distinct acellular assays (DTT and AA) on PM_{10} samples collected over a yearly time series from 14 diverse locations across France from 2013 to 2018 (Figure 4). Distinct positive redox activity towards the OP^{DTT} assay was observed for primary road traffic, biomass burning, dust, methanesulphonic acid (MSA)-rich, and primary biogenic sources. Conversely, biomass burning and road traffic sources exhibited significant activity solely for the OP^{AA} assay. The daily median contribution of each source to total OP^{DTT} emphasised the predominant influence of the primary road traffic source. Both biomass burning and road traffic sources contributed equally to the observed OP^{AA} (Weber et al., 2021). The OPv was found to be comparable between the French datasets and those obtained in Switzerland through the same sampling and laboratory procedures.

Consequently, residential biomass burning and road traffic stand out as the primary targets for prioritisation in significantly reducing OP of PM levels in Western Europe. In addition, these results suggest that strategies focused

solely on reducing the mass concentrations of PM may not effectively decrease OP of PM levels. If the oxidative potential is closely linked to significant health impacts, targeting specific sources of PM rather than overall PM mass could be a more efficient mitigation approach (Daellenbach et al., 2020; Weber et al., 2021).

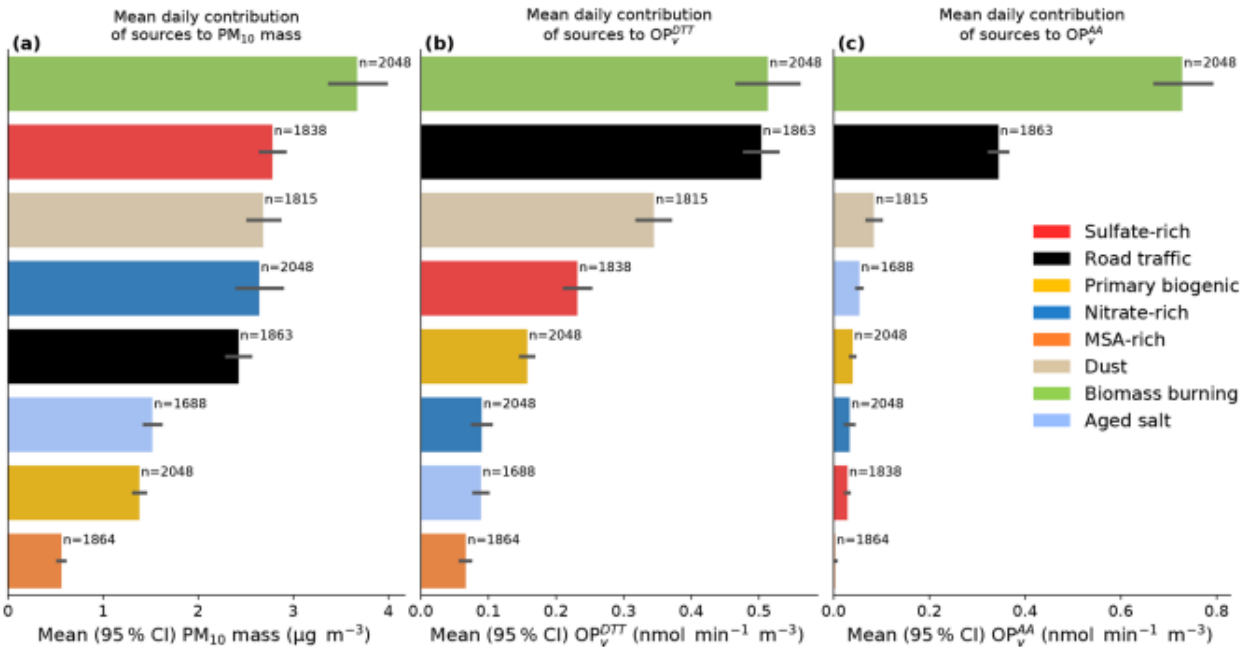

Figure 4. *Mean daily contribution of the sources to (a) the PM mass, (b) the $OP^{DTT}v$ and (c) the $OP^{AA}v$. The bars represent the mean, and the error bars represent the 95 % confidence interval of the mean(Weber et al., 2021).*

Despite the development of several acellular assays to evaluate OP of PM, there exists a lack of consensus regarding methodologies and protocols for the OP of PM measurement, as well as the quantification and calibration procedures, hindering inter-study comparisons. This lack of consensus is also related to the OP assays to be used to get a complete OP sensitivity, considering the dominance of PM sources at a specific site.

A recent study explored five distinct acellular OP assays and their sensitivity to the chemical composition of atmospheric PM_{10} and its emission sources collected at an urban alpine city in France (Dominutti et al., 2023). This included the assessment of well-established assays like AA, DTT, and DCFH, alongside novel assays such as Ferric-Xylenol Orange (FOX) and direct ROS quantification via OH radical. The main findings underscored the significant influence of seasonality on source contributions and OP activities. In winter, when anthropogenic emissions dominate, all OP assays exhibited strong agreement. Conversely, in warmer months, with reduced anthropogenic influence, biogenic and secondary organic-related aerosols exerted a greater impact. Additionally, we observed varying sensitivities of each OP assay to PM_{10} sources, likely reflecting differences in chemical composition and processes (Dominutti et al., 2023, Figure 5).

The results also emphasise the necessity of employing multiple OP assays to capture diverse sensitivities to redox-active species, providing deeper insights into the intrinsic capacity of PM sources to induce OP reactions. Given the heterogeneity of sources identified by different OP assays for a given ambient PM exposure, the selection of a single or combination of OP PM method(s) should be carefully considered as part of the assessment strategy. Such informed choices can provide valuable source-related information, guiding targeted reduction policies (Dominutti et al., 2023).

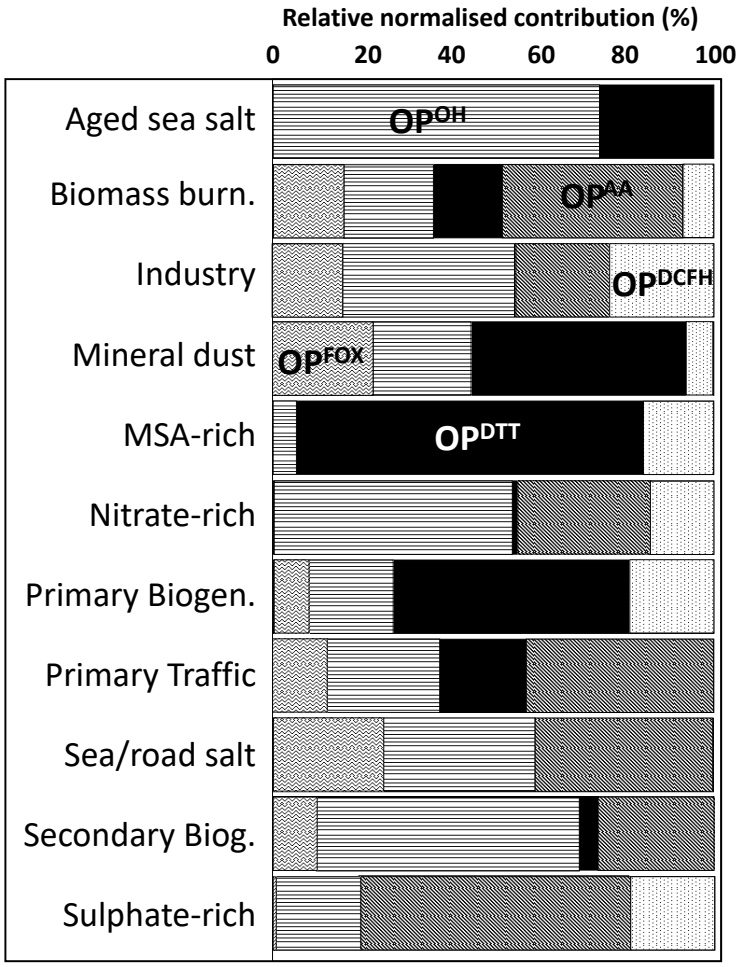

Figure 5. *OP sensitivity contribution of each PM source. Relative normalised contribution of OP assays to the PM_{10} sources Colours represent each OP test evaluated (adopted from Dominutti et al., 2023).*

4.2. Levels of OP in urban sites of Europe

4.1.1. France

In Grenoble (France), OP^{AA} of PM_{10} reached 2.38 ± 1.66 and 0.72 ± 0.39 nmol min^{-1} m^{-3} in winter and summer, respectively (Dominutti et al., 2023). In 14 French urban and traffic sites Weber (2021) and Weber et al. (2021) found OP^{AA} of PM_{10} values of 2.3±2.2 nmol min^{-1} m^{-3} in urban background with high biomass burning contributions, and 1.7±1.1 nmol min^{-1} m^{-3} in other urban background sites. For two traffic sites, the OP^{AA} of PM_{10} reached 2.1 and 1.3 nmol min^{-1} m^{-3}.

Likewise, in Grenoble (France), OP^{DTT} of PM_{10} reached 1.92 ± 1.31 and 1.46 ± 0.71 nmol min^{-1} m^{-3} in winter and summer, respectively (Dominutti et al., 2023). In 14 French urban and traffic sites Weber (2021) and Weber et al. (2021) found OP^{DTT} of PM_{10} values of 2.7–1.5 nmol min^{-1} m^{-3} for all urban background sites, with the exception of a high biomass burning urban valley, with 4.4 nmol min^{-1} m^{-3} and 2.6 and 2.4 nmol min^{-1} m^{-3} for the two traffic sites.

Dominutti et al. (2023) also found a good agreement with anthropogenic sources governing leading OP PM exposure (mainly biomass burning and primary traffic) for all five OP assays assessed during winter. However, this trend changes during warm months, with a reduction of the OP share of direct anthropogenic emissions and a higher impact from biogenic and secondary organic-related aerosols (anthropogenic and biogenic). Using PMF they

deduced that OP^{AA} and OP^{DTT} were mainly driven in the cold season by the following sources (nmol min^{-1} m^{-3}) in the order from largest source to the smallest source:

OP^{AA}: biomass burning (BB) > primary traffic PM >> sulphate-rich PM = Industrial> nitrate,
OP^{DTT}: BB >>primary traffic PM >> mineral dust > primary biogenic > methane sulphonic acid-rich;

while in the warm season these sources were from largest to smallest the following:

OP^{AA}: primary traffic PM >> secondary biogenic aerosols = sulphate-rich PM > BB = Industrial,
OP^{DTT}: methane sulphonic acid-rich >> mineral dust > primary biogenic > primary traffic >>BB = secondary biogenic.

Weber et al. (2021) evaluated the source contributions of OP^{AA} and OP^{DTT} of PM_{10} for 15 French cities using PMF and they found that normalised per µg of mass contribution of the different sources the following order of OP was found (nmol min^{-1} μg^{-1}):

OP^{AA}: BB > road traffic >>> aged sea salt = primary biogenic > mineral dust = sulphate-rich,
OP^{DTT}: road traffic >> primary biogenic = BB = methane sulphonic acid-rich = mineral dust > sulphate-rich >> aged sea salt = nitrate;

While considering the contribution of each source to averaged PM_{10} daily levels (on the contrary to the above), the following contribution was found (nmol min^{-1} m^{-3}):

OP^{AA}: **BB >> road traffic >>> mineral dust >>** aged sea salt = primary biogenic = nitrate-rich = sulphate-rich,
OP^{DTT}: **BB = road traffic >> mineral dust >** sulphate-rich >primary biogenic > aged sea salt = nitrate > methanesulphonic acid-rich.

Thus, biomass burning followed by road traffic and further with mineral dust were found to be the major sources of OP^{AA} and OP^{DTT}.

4.1.2. Greece

Paraskevopoulou et al. (2019) reported OP^{DTT} of $PM_{2.5}$ and PM_{10} ($PM_{2.5}$+$PM_{2.5-10}$) of 0.33 and 0.43 nmol min^{-1} m^{-3}, respectively, for an urban background site in Athens. They found that the OP^{DTT} was driven by

$$PM_{2.5}\ OP^{DTT} = 0.13 + 0.028*BBOA + 0.071*LV\text{-}OOA + 0.017*HOA\ (R^2=0.65)$$

were, BBOA, LV-OOA, HOA are the concentrations of biomass burning organic aerosol, low volatility secondary organic aerosol, and fossil fuel combustion (hydrocarbon-like) organic aerosols, respectively, in µg m^{-3}.

Argyropoulos et al. (2016) found for Thessaloniki OP^{DTT} values of 1.16 and 1.09 nmol min^{-1} m^{-3} for the cold and warm seasons in a traffic sites, and 3.10 and 0.84 nmol min^{-1} m^{-3} for the same seasons in an urban background site. They found that biomass burning was the main contributor to the high OP^{DTT} values reported for the urban background site in the cold season. In the traffic site traffic-related PM was the major driver.

4.1.3. Hungary

Vörösmarty et al. (2023) reported OP^{AA} of $PM_{2.5}$ of 2.4–2.1 nmol min^{-1} m^{-3} for urban and sub-urban sites of Budapest with the highest levels in the suburban site. For OP^{DTT} the values reached 2.9–1.9 nmol min^{-1} m^{-3}, with the highest values obtained in the urban site. They found that the OP^{AA} and OP^{DTT} were driven by:

Urban

$PM_{2.5}\ OP^{AA}$=1.07*BB + 0.36*road traffic + 0.14*industrial+0.03*dust+ 0.02*vehicle wear - 0.08 (R^2=0.86)
$PM_{2.5}\ OP^{DTT}$=0.79*BB + 0.89*road traffic + 0.49*oil comb +0.09*dust+ 0.09*vehicle wear - 0.36 (R^2=0.81)

Sub-urban

$PM_{2.5}$ OP^{AA}=0.79*BB + 0.57*dust + 0.52*oil comb + 0.17*industrial + - 0.47 (R^2=0.72)

$PM_{2.5}$ OP^{DTT}=0.97*oil comb + 0.62*BB + 0.18*road traffic + 0.09*industrial +0.02*dust - 0.50 (R^2=0.78)

4.1.4. Italy

Pietrogrande et al. (2019) reviewed the OP of PM_{10} and $PM_{2.5}$ studies carried out in urban and industrial sites in several Italian cities. They (and references therein) reported OP^{AA} of PM_{10} reaching 1.4, 0.7 and 0.2 nmol min^{-1} m^{-3} for industrial and urban Trentino, and urban Lecce, respectively. For OP^{DTT}, the values reached 0.6, 0.6 and 0.2 nmol min^{-1} m^{-3}, respectively. For $PM_{2.5}$, OP^{AA} reached 0.6 and 0.1 nmol min^{-1} m^{-3} for Bologna and Lecce, respectively. OP^{DTT} reached 0.8, 0.2 and 0.2 nmol min^{-1} m^{-3} for Bologna, Lecce and Trentino, respectively.

They found higher OP PM levels in winter compared to summer, especially when biomass burning influenced PM levels. Also, OP^{AA} was driven by industrial and road traffic metals, while OP^{DTT} was more affected by carbonaceous PM components.

Visentin et al. (2016) found that although both assays respond to the same redox-active species, i.e., quinones and transition metals, no correlations were found between OP^{DTT} and OP^{AA} responses to different standard compounds as well as to ambient samples highlighting that the sensitivity of each assay is different. OP^{DTT} in $PM_{2.5}$ was driven by metals (Cu, Zn, Cr, Fe, Ni, Mn), whereas OP^{AA} showed only moderate correlation with Cu and Mn.

4.1.5. Spain

In 't Veld et al. (2023) reported OP^{AA} of PM_{10} and $PM_{2.5}$ of 1.9 and 1.0, and 0.4 and 0.3 nmol $min^{-1}m^{-3}$, respectively, for urban and regional background sites of Barcelona. For OP^{DTT}, the values reached 2.5 and 1.2, and 0.5 and 0.4 nmol min^{-1} m^{-3}, respectively.

They also found that contributions from biomass burning to PM were very low, and that industry (metals), heavy oil combustion (V and Ni) and road traffic drove OP^{DTT} and OP^{AA} in PM_{10}, while road dust and industry contributed to $PM_{2.5}$ and industry to PM_1, although in all cases secondary organics also had an impact.

4.1.6. Switzerland

Grange et al. (2022) reported that OP^{AA} of PM_{10} reached 4.1–1.7 nmol min^{-1} m^{-3} and 1.6–1.7 nmol min^{-1} m^{-3} for $PM_{2.5}$ in four urban and sub-urban sites of Switzerland with the highest levels in the traffic site. Thus, OP^{AA} tends to be higher in the coarser fraction where metals from non-exhaust vehicle emissions are prominent. For OP^{DTT}, the values reached 3.0–0.8 and 1.0–0.6 nmol min^{-1} m^{-3}, respectively, and for OP^{DCFH} the values were 0.4–0.7 nmol min^{-1} m^{-3} for both fractions.

The same study, using multilinear regression (MLR) models, found that the combination of tracers of biomass burning (levoglucosan, galactosan, mannosan, K, OC, EC, depending on the site) and those from non-exhaust vehicle emissions (Fe, Cu, Sb, Mn) accounted for most of the OP^{AA} and OP^{DTT} in both PM_{10} and $PM_{2.5}$, with R^2=0.79- 0.97.

As examples of these MLR results some equations are listed:

Bern-Traffic site: PM_{10} OP^{AA}=109*galactosan + 319*Mn (R^2=89)

$PM_{2.5}$ OP^{AA}=18*mannosan + 107*Cu (R^2=90)

This indicates that for OP^{AA} higher weight is due to non-exhaust vehicle emissions (Cu, Mn) than from biomass burning (galactosan and mannosan).

PM_{10} OP^{DTT}= 2*EC + 0.85*NH_4^+ (R^2=80)

$PM_{2.5}$ OP^{DTT}= 31*galactosan + 475*Ti + 0.3*NH_4^+ (R^2=88)

This, on the other hand, indicates that for OP^{DTT} higher weight is due to exhaust vehicle emissions and road dust (Ti) than biomass burning (galactosan).

Basel-urban back. site PM_{10} OP^{AA}=96*galactosan + 130*Cu (R^2=96)
$PM_{2.5}$ OP^{AA}=2.5*levoglucosan + 614*Sb (R^2=88)

This indicates that for OP^{AA} higher weight is due to non-exhaust vehicle emissions (Cu, Sb) than from biomass burning (galactosan and levoglucosan) in the urban background site.

PM_{10} OP^{DTT}= 1.5*Fe + 0.44*NH_4^+ (R^2=90)
$PM_{2.5}$ OP^{DTT}= 31*galactosan + 129*Cu + 0.1*NH_4^+ (R^2=89)

Again, this similarly indicates that for OP^{DTT} higher weight is due to non-exhaust vehicle emissions (Fe, Cu) than from biomass burning (galactosan).

4.1.7. The Netherlands

Janssen et al. (2014) reported OP^{DTT} of PM_{10} reaching 3.7 and 2.6 and 1.7 nmol min^{-1} m^{-3} for two traffic sites and an urban background site in the Netherlands. For $PM_{2.5}$, the values reached 3.3, 1.7 and 1.4 nmol min^{-1} m^{-3}, respectively.

The OP^{ESR} and OP^{AA} were driven by traffic-related PM components (i.e. EC, Fe, Cu, PAHs), whereas OP^{DTT} was driven by PM mass and OC.

4.1.8. Synthesis

Figure 6 summarises the OP^{AA} and OP^{DTT} values in volume (nmol min^{-1} m^{-3}) from the studies reported for each country (Janssen et al., 2014; Argyropoulos et al., 2016; Visentin et al., 2016; Paraskevopoulou et al., 2019; Pietrogrande et al., 2019, and references therein; Weber, 2021; Weber et al., 2021; Grange et al., 2022; Dominutti et al., 2023; In 't Veld et al., 2023; Vörösmarty et al., 2023).

The following **comparison of OP values across urban Europe should be treated with caution**, as not all analyses were carried out using the same protocol. However, they do provide some indication of the levels observed in Europe and another publication will follow based on harmonised measurements to refine OP of PM European levels (Tassel et al., submitted to Nature on 24/10/2024).

The OP^{DTT} volume concentrations reached in PM_{10} from around 4.5 to 0.2 nmol min^{-1} m^{-3} in urban Europe. The highest values (>1.5 nmol min^{-1} m^{-3}) were obtained at traffic and urban background sites with high contributions of PM from biomass burning (e.g., Passy, Chamonix) or traffic-industry (e.g., Barcelona, Marseille). Sites receiving PM influenced by high traffic and biomass burning recorded OP^{DTT} values around 2.5 nmol min^{-1} m^{-3}, while most of the other reached around 1.7 nmol min^{-1} m^{-3}. A number of urban background sites reached lower values, from 1.5 to 0.2 nmol min^{-1} m^{-3}. In $PM_{2.5}$, these values reached from 3.3 to 0.2 nmol min^{-1} m^{-3}, with the highest values in a traffic and an urban background site in Budapest, however, most of the traffic and urban background sites fell in the range of 2.0 to 0.5 nmol min^{-1} m^{-3}.

For OP^{AA} of PM_{10} very similar trends to those reported for OP^{DTT} were evidenced, with the highest values obtained for two traffic sites (4.1-2.9 nmol min^{-1} m^{-3}) and most urban background and traffic sites reaching values from 2.5 to 1.0 nmol min^{-1} m^{-3}, again with the highest values of urban background locations recorded in the cities with essentially high traffic and/or biomass burning contributions. In $PM_{2.5}$, the values decreased a lot compared with PM_{10}, specially for traffic sites, probably because OP^{AA} is highly influenced by metals from non-exhaust vehicle PM emissions, that are markedly reduced in $PM_{2.5}$ compared to PM_{10}.

All these results point out that both OP^{AA} and OP^{DTT} are sensitive to organic species and metals carried out by PM but in a different extent. In fact, OP^{DTT} – a thiol-based assay, displays a more balanced response to all atmospheric compounds than OP^{AA}, being more specific to a few specific species (mainly metallic, or biomass-burning compounds related).

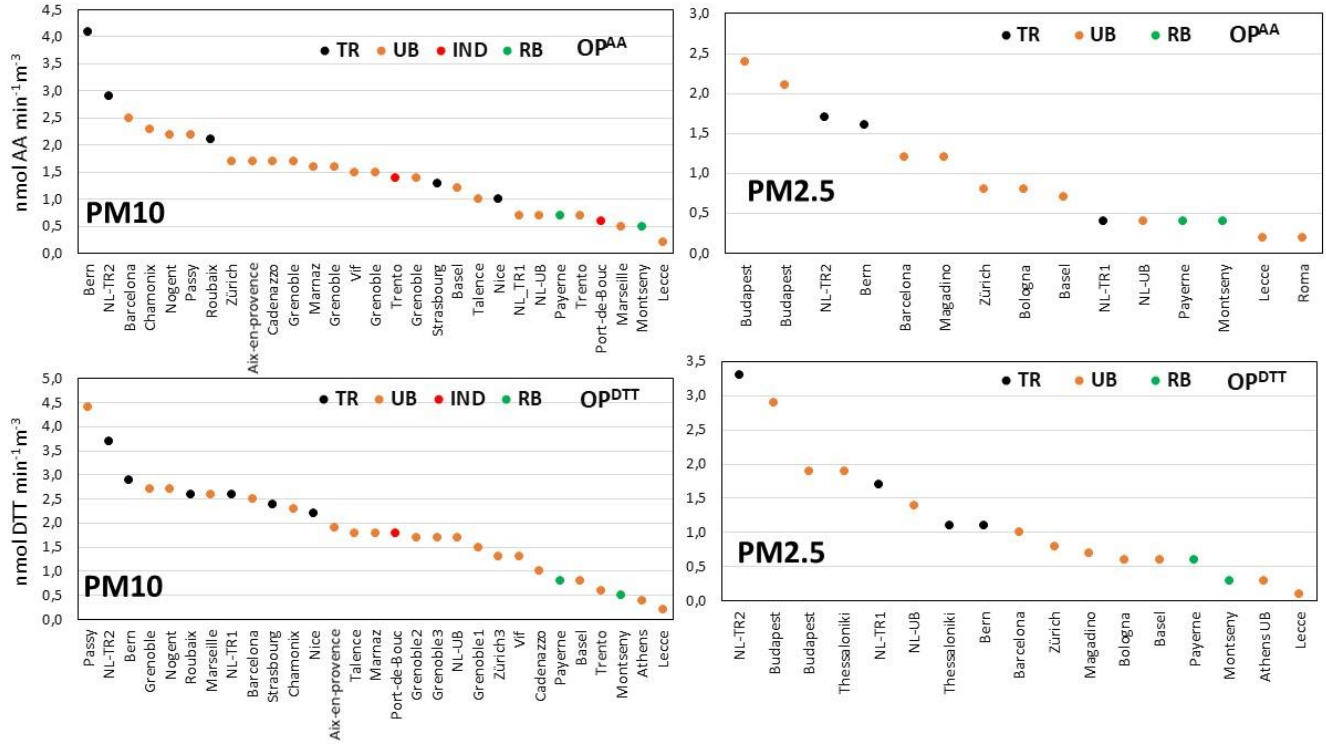

Figure 6. *OP^{AA} and OP^{DTT} volume of PM mean values (nmol min^{-1} m^{-3}) in (mostly) urban sites, reported by Janssen et al. (2014), Argyropoulos et al. (2016), Visentin et al. (2016), Paraskevopoulou et al. (2019), Pietrogrande et al. (2019, and references therein), Weber (2021), Weber et al. (2021), Grange et al. (2022), Dominutti et al. (2023), In 't Veld et al. (2023) and Vörösmarty et al. (2023).*

5. GENERAL RECOMMENDATIONS FOR FURTHER STANDARDISATION OF OTHER PROTOCOLS FOR OXIDATIVE POTENTIAL OF PM

Based on the findings of the RI-URBANS' interlaboratory comparison, some recommendations for further standardising OP protocols are suggested. These include guidelines for samples preparation and laboratory conditions, instrument calibration and report of results. Additionally, a reference material (naphthoquinone, copper or other solution at a known concentration) for OP of PM measurement should be proposed to facilitate interlaboratory comparisons. Additionally, even if some differences were observed in the results obtained from the use of the RI-URBANS's simplified SOP, harmonisation of procedures is needed to ensure data comparability (Dominutti et al., 2024). We describe below the crucial points that matter in OP of PM evaluation and need to be considered for the harmonisation of OP assays in general. In fact, in absence of a clear link between epidemiological studies and a single or a specific set of OP assays, the development and testing of various OP assays with wider sensitivities to redox active species should continue.

5.2.1. The selection of the assay for oxidative potential of PM

To date, two complementary OP assays, a thiol-based probe (OP^{DTT} or OP^{GSH}) and another one (among OP^{OH}, OP^{AA}, or else), are recommended to provide a better picture of the potential oxidising damages from PM compounds and

to strengthen the power of epidemiological studies. In fact, the choice of the best OP test (or combination) must be based on epidemiological evidence which have only recently been studied and which need more hindsight to be determined.

5.2.2. Storage of the samples

PM samples should be immediately transported to the laboratory after sampling. There filters must be kept cold after sampling (at or below 4°C if the OP analysis is done within a few days after collection or <-20°C if the analysis is delayed). The lifetime of the ROS may be very short, and measurements on filters are affected over time. Ageing studies should be performed for each OP assay in the long term to define the maximum time of storage in cold and ambient conditions for aerosol filters.

5.2.3. Laboratory conditions

OP assays are "trace" assays that require clean ambient conditions for handling, such as a clean room or laminar flow bench, to prevent contamination of the samples. It is also recommended to use thoroughly cleaned materials; vials, cones and spatulas must be washed before use using acidic bath and rinsing with ultra-pure water). Finally, the laboratory temperatures and light exposure should be measured and controlled.

5.2.4. Sample extraction for the assay

The extraction step may be highly variable according to procedures, and several parameters are known to impact OP of PM results, such as the choice of the solvent, the concentration of buffer, the way of agitation and the concentration of PM sample extraction. We recommend that all these parameters need to be explicitly controlled and harmonised for each OP test developed

5.2.5. Reaction stage of the assay

Several aspects of the reaction process affect the OP PM value such as the initial concentration of reactants, ratio reactant/sample, time of reaction, temperature of reaction and the type of measures (kinetic or end-point value). Current literature mainly addresses extraction or reaction parameters separately. We advise that both factors be evaluated together to quantify their relative impact on the results so as to formulate recommendations.

5.2.6. Development of a reference material with a certified "OP PM value"

The use of a reference material with an associated OP PM value could help some laboratories to test and train themselves on the OP protocol before testing the blind samples.

5.2.7. Instrument calibration

Investigate the optimal frequency for the calibration of spectrophotometers for such assays

5.2.8. Report of results

The calculation of OP^{DTT} activity during the RI-URBANS' SOP involved a conversion using a calibration curve. For future comparison exercises, the report of the results requires also some standardisation and the possibility of exploring alternative methods for OP calculation should be tested.

5.2.9. Measurement of OP in EU air quality supersites

This Service Tools highlights the complexity of setting up correct measurements of OP from atmospheric filters. It is a kinetic measurement that can be affected by various laboratory and experimental conditions, if there are not harmonised. The OP measurements recommended at EU air quality supersites are intended to provide long-term time-series to epidemiological studies, therefore the EU-scale harmonisation is crucial. That being said, as long as OP is not operated online, for filter OP measurements at EU Urban sites, we recommend choosing laboratories with experience on OP of PM and concentrating measurements as much as possible in a limited number of laboratories per country.

6. REFERENCES

Abrams, J.Y., Weber, R.J., Klein, M., Samat, S.E., Chang, H.H., Strickland, M.J., Verma, V., Fang, T., Bates, J.T., Mulholland, J.A., Russell, A.G., Tolbert, P.E., 2017. Associations between Ambient Fine Particulate Oxidative Potential and Cardiorespiratory Emergency Department Visits. Environ. Health Perspect. 125, 107008. https://doi.org/10.1289/EHP1545

Bates, J.T., Fang, T., Verma, V., Zeng, L., Weber, R.J., Tolbert, P.E., Abrams, J.Y., Sarnat, S.E., Klein, M., Mulholland, J.A., Russell, A.G., 2019. Review of Acellular Assays of Ambient Particulate Matter Oxidative Potential: Methods and Relationships with Composition, Sources, and Health Effects. Environ. Sci. Technol. 53, 4003–4019. https://doi.org/10.1021/acs.est.8b03430

Bates, J.T., Weber, R.J., Abrams, J., Verma, V., Fang, T., Klein, M., Strickland, M.J., Sarnat, S.E., Chang, H.H., Mulholland, J.A., Tolbert, P.E., Russell, A.G., 2015. Reactive Oxygen Species Generation Linked to Sources of Atmospheric Particulate Matter and Cardiorespiratory Effects. Environ. Sci. Technol. 49, 13605–13612. https://doi.org/10.1021/acs.est.5b02967

Borlaza, L.J.S., Uzu, G., Ouidir, M., Lyon-Caen, Sarah, Marsal, A., Weber, S., Siroux, Valérie, Lepeule, Johanna, Boudier, A., Jaffrezo, J.-L., Slama, Rémy, Lyon-Caen, S., Siroux, V., Lepeule, J., Philippat, C., Slama, R., Hofmann, P., Hullo, E., Llerena, C., Quentin, J., Pin, I., Eyriey, E., Licinia, A., Vellement, A., Morin, X., Morlot, A., the SEPAGES cohort study group, 2022. Personal exposure to PM2.5 oxidative potential and its association to birth outcomes. J. Expo. Sci. Environ. Epidemiol. https://doi.org/10.1038/s41370-022-00487-w

Borlaza, L.J.S., Weber, S., Jaffrezo, J.-L., Houdier, S., Slama, R., Rieux, C., Albinet, A., Micallef, S., Trébluchon, C., Uzu, G., 2021. Disparities in particulate matter (PM₁₀) origins and oxidative potential at a city scale (Grenoble, France) – Part 2: Sources of PM₁₀ oxidative potential using multiple linear regression analysis and the predictive applicability of multilayer perceptron neural network analysis. Atmospheric Chem. Phys. 21, 9719–9739. https://doi.org/10.5194/acp-21-9719-2021

Borlaza-Lacoste, L., Mardoñez, V., Marsal, A., Hough, I., Dinh, V.N.T., Dominutti, P., Jaffrezo, J.-L., Alastuey, A., Besombes, J.-L., Močnik, G., Moreno, I., Velarde, F., Gardon, J., Cornejo, A., Andrade, M., Laj, P., Uzu, G., 2024. Oxidative potential of particulate matter and its association to respiratory health endpoints in high-altitude cities in Bolivia. Environ. Res. 255, 119179. https://doi.org/10.1016/j.envres.2024.119179

Calas, A., Uzu, G., Besombes, J.L., Martins, J.M.F., Redaelli, M., Weber, S., Charron, A., Albinet, A., Chevrier, F., Brulfert, G., Mesbah, B., Favez, O., Jaffrezo, J.L., 2019. Seasonal variations and chemical predictors of oxidative potential (OP) of particulate matter (PM), for seven urban French sites. Atmosphere 10, 1–20. https://doi.org/10.3390/atmos10110698

Calas, A., Uzu, G., Kelly, F.J., Houdier, S., Martins, J.M.F., Thomas, F., Molton, F., Charron, A., Dunster, C., Oliete, A., Jacob, V., Besombes, J.-L., Chevrier, F., Jaffrezo, J.-L., 2018. Comparison between five acellular oxidative potential measurement assays performed with detailed chemistry on PM10 samples from the city of Chamonix (France). Atmospheric Chem. Phys. 18, 7863–7875. https://doi.org/10.5194/acp-18-7863-2018

Calas, A., Uzu, G., Martins, J.M.F., Voisin, D., Spadini, L., Lacroix, T., Jaffrezo, J.-L., 2017. The importance of simulated lung fluid (SLF) extractions for a more relevant evaluation of the oxidative potential of particulate matter. Sci. Rep. 7, 11617. https://doi.org/10.1038/s41598-017-11979-3

Canova Cristina, Minelli Cosetta, Dunster Christina, Kelly Frank, Shah Pallav, Caneja Cielito, Tumilty Michael, Burney Peter, 2014. PM10 Oxidative Properties and Asthma and COPD. Epidemiology, Letters 25. https://doi.org/10.1097/EDE.0000000000000085

Cesari, D., Merico, E., Grasso, F.M., Decesari, S., Belosi, F., Manarini, F., Nuntiis, P.D., Rinaldi, M., Volpi, F., Gambaro, A., Morabito, E., Contini, D., 2019. Source Apportionment of PM2.5 and of its Oxidative Potential in an Industrial Suburban Site in South Italy. Atmosphere 10, 758. https://doi.org/10.3390/atmos10120758

Cho, A.K., Sioutas, C., Miguel, A.H., Kumagai, Y., Schmitz, D.A., Singh, M., Eiguren-Fernandez, A., Froines, J.R., 2005. Redox activity of airborne particulate matter at different sites in the Los Angeles Basin. Environ. Res. 99, 40–47. https://doi.org/10.1016/j.envres.2005.01.003

Daellenbach, K.R., Uzu, G., Jiang, J., Cassagnes, L.-E., Leni, Z., Vlachou, A., Stefenelli, G., Canonaco, F., Weber, S., Segers, A., Kuenen, J.J.P., Schaap, M., Favez, O., Albinet, A., Aksoyoglu, S., Dommen, J., Baltensperger, U.,

Geiser, M., El Haddad, I., Jaffrezo, J.-L., Prévôt, A.S.H., 2020. Sources of particulate-matter air pollution and its oxidative potential in Europe. Nature 587, 414–419. https://doi.org/10.1038/s41586-020-2902-8

Delfino, R.J., Sioutas, C., Malik, S., 2005. Potential role of ultrafine particles in associations between airborne particle mass and cardiovascular health. Environ. Health Perspect. 113, 934–946. https://doi.org/10.1289/ehp.7938

Dominutti, P., Borlaza, L.J.S., Sauvain, J.-J., Ngoc Thuy, Vy Dinh, Houdier, S., Da, G., Jaffrezo, J.L., Tobin, S., Trébuchon, C., Socquet, S., Moussu, E., Mary, G., Uzu, Gaelle, G., 2023. Source apportionment of oxidative potential depends on the choice of the assay: insights into 5 protocols comparison and implications for mitigation measures. Environ. Sci. Atmospheres,3, 1497, https://doi.org/10.1039/D3EA00007A

Dominutti, P., Jaffrezo, J.L., Bougiatioti, K., Campbell, S.J., Cavalli, F., Contini, D., Evans, G.J., Harrison, R.M., Hoek, G., Jovanovic, M., Kalberer, M., Kooter, I., Mihalopoulos, N., Mikuska, P., Mudway, I.S., Nenes, A., Paulson, S.E., Paraskevopoulou, D., Pietrogrande, M.C., Putaud, J.P., Querol, X., Sauvain, J.J., Shahpoury, P., Steimer, S.S., Stevanović, S., Verma, V., Weber, J.R., Uzu, G., 2024. An interlaboratory comparison of oxidative potential measurement: challenges and recommendations for harmonisation. Atmo. Meas. Tech., 24, 107. Under discussion, https://doi.org/10.5194/amt-2024-107

Fang, T., Guo, H., Zeng, L., Verma, V., Nenes, A., Weber, R.J., 2017a. Highly Acidic Ambient Particles, Soluble Metals, and Oxidative Potential: A Link between Sulfate and Aerosol Toxicity. Environ. Sci. Technol. 51, 2611–2620. https://doi.org/10.1021/acs.est.6b06151

Fang, T., Verma, V., Bates, J.T., Abrams, J., Klein, M., Strickland, J.M., Sarnat, E.S., Chang, H.H., Mulholland, A.J., Tolbert, E.P., Russell, G.A., Weber, J.R., 2016. Oxidative potential of ambient water-soluble PM2.5 in the southeastern United States: Contrasts in sources and health associations between ascorbic acid (AA) and dithiothreitol (DTT) assays. Atmospheric Chem. Phys. 16, 3865–3879. https://doi.org/10.5194/acp-16-3865-2016

Fang, T., Zeng, L., Gao, D., Verma, V., Stefaniak, A.B., Weber, R.J., 2017b. Ambient Size Distributions and Lung Deposition of Aerosol Dithiothreitol-Measured Oxidative Potential: Contrast between Soluble and Insoluble Particles. Environ. Sci. Technol. 51, 6802–6811. https://doi.org/10.1021/acs.est.7b01536

Gao, D., Mulholland, J.A., Russell, A.G., Weber, R.J., 2020. Characterization of water-insoluble oxidative potential of PM2.5 using the dithiothreitol assay. Atmos. Environ. 224, 117327. https://doi.org/10.1016/j.atmosenv.2020.117327

Goldsmith, C.-A., Frevert, C., Imrich, A., Sioutas, C., Kobzik, L., 1997. Alveolar Macrophage Interaction with Air Pollution Particulates. Environ. Health Perspect. 105, 1191. https://doi.org/10.2307/3433531

Grandesso, E., Kowalewski, K., Perez Ballesta, P., 2012. First EC-JRC PAHs inter-laboratory comparison on PM10 quartz filters. (No. EUR 25170 EN-2012). European Commission. Joint Research Centre. Institute for Environment and Sustainability., Luxembourg.

Grange, S.K., Uzu, G., Weber, S., Jaffrezo, J., Hueglin, C., 2022. Linking Switzerland's PM;10 and PM2.5 oxidative potential (OP) with emission sources. Atmospheric Chem. Phys. 22, 7029–7050. https://doi.org/10.5194/acp-22-7029-2022

Gulliver, J., Morley, D., Dunster, C., McCrea, A., van Nunen, E., Tsai, M.-Y., Probst-Hensch, N., Eeftens, M., Imboden, M., Ducret-Stich, R., Naccarati, A., Galassi, C., Ranzi, A., Nieuwenhuijsen, M., Curto, A., Donaire-Gonzalez, D., Cirach, M., Vermeulen, R., Vineis, P., Hoek, G., Kelly, F.J., 2018. Land use regression models for the oxidative potential of fine particles (PM 2.5) in five European areas. Environ. Res. 160, 247–255. https://doi.org/10.1016/j.envres.2017.10.002

He, L., Norris, C., Cui, X., Li, Z., Barkjohn, K.K., Brehmer, C., Teng, Y., Fang, L., Lin, L., Wang, Q., Zhou, X., Hong, J., Li, F., Zhang, Y., Schauer, J.J., Black, M., Bergin, M.H., Zhang, J.J., 2021. Personal Exposure to PM $_{2.5}$ Oxidative Potential in Association with Pulmonary Pathophysiologic Outcomes in Children with Asthma. Environ. Sci. Technol. 55, 3101–3111. https://doi.org/10.1021/acs.est.0c06114

Hellack, B., Yang, A., Cassee, F.R., Janssen, N.A.H., Schins, R.P.F., Kuhlbusch, T.A.J., 2014. Intrinsic hydroxyl radical generation measurements directly from sampled filters as a metric for the oxidative potential of ambient particulate matter. J. Aerosol Sci. 72, 47–55. https://doi.org/10.1016/j.jaerosci.2014.02.003

in 't Veld, M., Pandolfi, M., Amato, F., Pérez, N., Reche, C., Dominutti, P., Jaffrezo, J., Alastuey, A., Querol, X., Uzu, G., 2023. Discovering oxidative potential (OP) drivers of atmospheric PM10, PM2.5, and PM1 simultaneously in North-Eastern Spain. Sci. Total Environ. 857, 159386. https://doi.org/10.1016/j.scitotenv.2022.159386

Janssen, N.A.H., Strak, M., Yang, A., Hellack, B., Kelly, F.J., Kuhlbusch, T.A.J., Harrison, R.M., Brunekreef, B., Cassee, F.R., Steenhof, M., Hoek, G., 2015. Associations between three specific a-cellular measures of the oxidative potential of particulate matter and markers of acute airway and nasal inflammation in healthy volunteers. Occup. Environ. Med. 72, 49–56. https://doi.org/10.1136/oemed-2014-102303

Korsiak, J., Lavigne, E., You, H., Pollitt, K., Kulka, R., Hatzopoulou, M., Evans, G., Burnett, R.T., Weichenthal, S., 2022. Air Pollution and Pediatric Respiratory Hospitalizations: Effect Modification by Particle Constituents and Oxidative Potential. Am. J. Respir. Crit. Care Med. 206, 1370–1378. https://doi.org/10.1164/rccm.202205-0896OC

Landreman, A.P., Shafer, M.M., Hemming, J.C., Hannigan, M.P., Schauer, J.J., 2008. A Macrophage-Based Method for the Assessment of the Reactive Oxygen Species (ROS) Activity of Atmospheric Particulate Matter (PM) and Application to Routine (Daily-24 h) Aerosol Monitoring Studies. Aerosol Sci. Technol. 42, 946–957. https://doi.org/10.1080/02786820802363819

Lavigne, É., Burnett, R.T., Stieb, D.M., Evans, G.J., Godri Pollitt, K.J., Chen, H., van Rijswijk, D., Weichenthal, S., 2018. Fine Particulate Air Pollution and Adverse Birth Outcomes: Effect Modification by Regional Nonvolatile Oxidative Potential. Environ. Health Perspect. 126, 077012. https://doi.org/10.1289/EHP2535

Liu, L., Urch, B., Szyszkowicz, M., Evans, G., Speck, M., Van Huang, A., Leingartner, K., Shutt, R.H., Pelletier, G., Gold, D.R., Brook, J.R., Godri Pollitt, K., Silverman, F.S., 2018. Metals and oxidative potential in urban particulate matter influence systemic inflammatory and neural biomarkers: A controlled exposure study. Environ. Int. 121, 1331–1340. https://doi.org/10.1016/j.envint.2018.10.055

Maikawa, C.L., Weichenthal, S., Wheeler, A.J., Dobbin, N.A., Smargiassi, A., Evans, G., Liu, L., Goldberg, M.S., Pollitt, K.J.G., 2016. Particulate Oxidative Burden as a Predictor of Exhaled Nitric Oxide in Children with Asthma. Environ. Health Perspect. 124, 1616–1622. https://doi.org/10.1289/EHP175

Marsal, A., Sauvain, J.-J., Thomas, A., Lyon-Caen, S., Borlaza, L.J.S., Philippat, C., Jaffrezo, J.-L., Boudier, A., Darfeuil, S., Elazzouzi, R., Lepeule, J., Chartier, R., Bayat, S., Slama, R., Siroux, V., Uzu, G., 2024. Effects of personal exposure to the oxidative potential of PM2.5 on oxidative stress biomarkers in pregnant women. Sci. Total Environ. 911, 168475. https://doi.org/10.1016/j.scitotenv.2023.168475

Marsal, A., Slama, R., Lyon-Caen, S., Borlaza, L.J.S., Jaffrezo, J.-L., Boudier, A., Darfeuil, S., Elazzouzi, R., Gioria, Y., Lepeule, J., Chartier, R., Pin, I., Quentin, J., Bayat, S., Uzu, G., Siroux, V., the SEPAGES cohort study group, 2023. Prenatal Exposure to PM2.5 Oxidative Potential and Lung Function in Infants and Preschool- Age Children: A Prospective Study. Environ. Health Perspect. 131, 017004. https://doi.org/10.1289/EHP11155

Massimi, L., Ristorini, M., Astolfi, M.L., Perrino, C., Canepari, S., 2020. High resolution spatial mapping of element concentrations in PM10: A powerful tool for localization of emission sources. Atmospheric Res. 244, 105060. https://doi.org/10.1016/j.atmosres.2020.105060

Paraskevopoulou, D., Bougiatioti, A., Stavroulas, I., Fang, T., Lianou, M., Liakakou, E., Gerasopoulos, E., Weber, R., Nenes, A., Mihalopoulos, N., 2019. Yearlong variability of oxidative potential of particulate matter in an urban Mediterranean environment. Atmos. Environ. 206, 183–196. https://doi.org/10.1016/j.atmosenv.2019.02.027

Perrone, M.G., Zhou, J., Malandrino, M., Sangiorgi, G., Rizzi, C., Ferrero, L., Dommen, J., Bolzacchini, E., 2016. PM chemical composition and oxidative potential of the soluble fraction of particles at two sites in the urban area of Milan, Northern Italy. Atmos. Environ. 128, 104–113. https://doi.org/10.1016/j.atmosenv.2015.12.040

Pietrogrande, M.C., Dalpiaz, C., Dell'Anna, R., Lazzeri, P., Manarini, F., Visentin, M., Tonidandel, G., 2018. Chemical composition and oxidative potential of atmospheric coarse particles at an industrial and urban background site in the alpine region of northern Italy. Atmos. Environ. 191, 340–350. https://doi.org/10.1016/j.atmosenv.2018.08.022

Sarnat, S.E., Chang, H.H., Weber, R.J., 2016. Ambient PM2.5 and Health: Does PM2.5 Oxidative Potential Play a Role? Am. J. Respir. Crit. Care Med. 194, 530–531. https://doi.org/10.1164/rccm.201603-0589ED

Sauvain, J.J., Deslarzes, S., Riediker, M., 2008. Nanoparticle reactivity toward dithiothreitol. Nanotoxicology 2, 121–129. https://doi.org/10.1080/17435390802245716

Shahpoury, P., Zhang, Z.W., Filippi, A., Hildmann, S., Lelieveld, S., Mashtakov, B., Patel, B.R., Traub, A., Umbrio, D., Wietzoreck, M., Wilson, J., Berkemeier, T., Celo, V., Dabek-Zlotorzynska, E., Evans, G., Harner, T., Kerman, K., Lammel, G., Noroozifar, M., Pöschl, U., Tong, H., 2022. Inter-comparison of oxidative potential metrics for airborne particles identifies differences between acellular chemical assays. Atmospheric Pollut. Res. 13, 101596. https://doi.org/10.1016/j.apr.2022.101596

Shen, J., Taghvaee, S., La, C., Oroumiyeh, F., Liu, J., Jerrett, M., Weichenthal, S., Del Rosario, I., Shafer, M.M., Ritz, B., Zhu, Y., Paulson, S.E., 2022. Aerosol Oxidative Potential in the Greater Los Angeles Area: Source Apportionment and Associations with Socioeconomic Position. Environ. Sci. Technol. 56, 17795–17804. https://doi.org/10.1021/acs.est.2c02788

Shi, T., 2003. Temporal variation of hydroxyl radical generation and 8-hydroxy-2'-deoxyguanosine formation by coarse and fine particulate matter. Occup. Environ. Med. 60, 315–321. https://doi.org/10.1136/oem.60.5.315

Srivastava, D., Tomaz, S., Favez, O., Lanzafame, G.M., Golly, B., Besombes, J.-L., Alleman, L.Y., Jaffrezo, J.-L., Jacob, V., Perraudin, E., Villenave, E., Albinet, A., 2018. Speciation of organic fraction does matter for source apportionment. Part 1: A one-year campaign in Grenoble (France). Sci. Total Environ. 624, 1598–1611. https://doi.org/10.1016/j.scitotenv.2017.12.135

Strak, M., Janssen, N., Beelen, R., Schmitz, O., Karssenberg, D., Houthuijs, D., van den Brink, C., Dijst, M., Brunekreef, B., Hoek, G., 2017. Associations between lifestyle and air pollution exposure: Potential for confounding in large administrative data cohorts. Environ. Res. 156, 364–373. https://doi.org/10.1016/j.envres.2017.03.050

Toyib, O., Lavigne, E., Traub, A., Umbrio, D., You, H., Ripley, S., Pollitt, K., Shin, T., Kulka, R., Jessiman, B., Tjepkema, M., Martin, R., Stieb, D.M., Hatzopoulou, M., Evans, G., Burnett, R.T., Weichenthal, S., 2022. Long-term Exposure to Oxidant Gases and Mortality: Effect Modification by PM2.5 Transition Metals and Oxidative Potential. Epidemiology 33, 767–776. https://doi.org/10.1097/EDE.0000000000001538

Uzu, G., Sauvain, J.J., Baeza-Squiban, A., Riediker, M., Hohl, M.S.S., Val, S., Tack, K., Denys, S., Pradère, P., Dumat, C., 2011. In vitro assessment of the pulmonary toxicity and gastric availability of lead-rich particles from a lead recycling plant. Environ. Sci. Technol. 45, 7888–7895. https://doi.org/10.1021/es200374c

Verlhac, S., Leoz, E., Albinet, A., Cabillic, J., Lalere, B., Fallot, C., 2014. Comparaison interlaboratoires sur l'analyse des HAP dans l'air ambiant (No. DRC-14-144350-09750A). Laboratoire Central de Surveillance de la Qualité de l'Air.

Verma, V., Fang, T., Guo, H., King, L., Bates, J.T., Peltier, R.E., Edgerton, E., Russell, A.G., Weber, R.J., 2014. Reactive oxygen species associated with water-soluble PM_{2.5} in the southeastern United States: spatiotemporal trends and source apportionment. Atmospheric Chem. Phys. 14, 12915–12930. https://doi.org/10.5194/acp-14-12915-2014

Weber, S., Salameh, D., Albinet, A., Alleman, L.Y., Waked, A., Besombes, J.L., Jacob, V., Guillaud, G., Meshbah, B., Rocq, B., Hulin, A., Dominik-Sègue, M., Chrétien, E., Jaffrezo, J.L., Favez, O., 2019. Comparison of PM10 sources profiles at 15 french sites using a harmonized constrained positive matrix factorization approach. Atmosphere 10, 1–22. https://doi.org/10.3390/atmos10060310

Weber, S., Uzu, G., Calas, A., Chevrier, F., Besombes, J.-L., Charron, A., Salameh, D., Ježek, I., Močnik, G., Jaffrezo, J.-L., 2018. An apportionment method for the oxidative potential of atmospheric particulate matter sources: application to a one-year study in Chamonix, France. Atmospheric Chem. Phys. 18, 9617–9629. https://doi.org/10.5194/acp-18-9617-2018

Weber, S., Uzu, G., Favez, O., Borlaza, L.J.S., Calas, A., Salameh, D., Chevrier, F., Allard, J., Besombes, J.-L., Albinet, A., Pontet, S., Mesbah, B., Gille, G., Zhang, S., Pallares, C., Leoz-Garziandia, E., Jaffrezo, J.-L., 2021. Source apportionment of atmospheric PM10 oxidative potential: synthesis of 15 year-round urban datasets in France. Atmospheric Chem. Phys. 21, 11353–11378. https://doi.org/10.5194/acp-21-11353-2021

Weichenthal, S., Lavigne, E., Evans, G., Pollitt, K., Burnett, R.T., 2016. Ambient PM2.5 and risk of emergency room visits for myocardial infarction: impact of regional PM2.5 oxidative potential: a case-crossover study. Environ. Health 15, 46. https://doi.org/10.1186/s12940-016-0129-9

Xiong, Q., Yu, H., Wang, R., Wei, J., Verma, V., 2017. Rethinking Dithiothreitol-Based Particulate Matter Oxidative Potential: Measuring Dithiothreitol Consumption versus Reactive Oxygen Species Generation. Environ. Sci. Technol. 51, 6507–6514. https://doi.org/10.1021/acs.est.7b01272

Yang, A., Janssen, N.A.H., Brunekreef, B., Cassee, F.R., Hoek, G., Gehring, U., 2016. Children's respiratory health and oxidative potential of PM $_{2.5}$: the PIAMA birth cohort study. Occup. Environ. Med. 73, 154–160. https://doi.org/10.1136/oemed-2015-103175

Yang, A., Jedynska, A., Hellack, B., Kooter, I., Hoek, G., Brunekreef, B., Kuhlbusch, T.A.J., Cassee, F.R., Janssen, N.A.H., 2014. Measurement of the oxidative potential of PM2.5 and its constituents: The effect of extraction solvent and filter type. Atmos. Environ. 83, 35–42. https://doi.org/10.1016/j.atmosenv.2013.10.049

Zhou, J., Elser, M., Huang, R.-J., Krapf, M., Fröhlich, R., Bhattu, D., Stefenelli, G., Zotter, P., Bruns, E.A., Pieber, S.M., Ni, H., Wang, Q., Wang, Y., Zhou, Y., Chen, C., Xiao, M., Slowik, J.G., Brown, S., Cassagnes, L.-E., Daellenbach, K.R., Nussbaumer, T., Geiser, M., Prévôt, A.S.H., El-Haddad, I., Cao, J., Baltensperger, U., Dommen, J., 2019. Predominance of secondary organic aerosol to particle-bound reactive oxygen species activity in fine ambient aerosol. Atmospheric Chem. Phys. 19, 14703–14720. https://doi.org/10.5194/acp-19-14703-2019